ENGINEERING EXPERIMENT STATION
COLLEGE OF ENGINEERING

SHORT TERM MONITORING AND PERFORMANCE EVALUATION OF SOLAR DOMESTIC HOT WATER SYSTEMS

BY

WARREN ELLIOTT BUCKLES

MASTER OF SCIENCE
(MECHANICAL ENGINEERING)

UNIVERSITY OF WISCONSIN-MADISON

1983

APPROVED

William A. Beckman, Professor of Mechanical Engineering

July 18, 1983

SHORT TERM MONITORING

AND

PERFORMANCE EVALUATION

OF

SOLAR DOMESTIC HOT WATER SYSTEMS

BY

WARREN ELLIOTT BUCKLES

A thesis submitted in partial fulfillment of the
requirements for the degree of

MASTER OF SCIENCE
(Mechanical Engineering)

at the

UNIVERSITY OF WISCOSIN-MADISON

1983

ACKNOWLEDGEMENTS

The contributions of a great many people have helped to make this work possible.

My mother, Katarine Buckles (1918-1971), gave me her fascination with the way things work and her love of learning for its own sake.

Professors J. A. Duffie, W. A. Beckman and S. A. Klein of the University of Wisconsin Solar Energy Laboratory provided me with the facilities, ideas and encouragement necesary to complete this work.

Wendy Rakower, my wife, gave me her love and support.

The Madison Gas and Electric Company provided the financial resources necessary to carry out this work as well as supplying the technical support needed to test their solar domestic hot water system.

Finally, I would like to thank Tom Pynchon for not forgetting the Kenosha Kid.

ABSTRACT

The development of a short term in situ testing methodology suitable for testing solar domestic hot water (SDHW) systems is described. The design of a low-cost data acquisition system suitable for testing SDHW systems is detailed. Test data from two systems in the Madison area is presented.

The methodology involves a one-day or more test cycle in which tank losses and collector loop performance are measured. The measure collector loop performance includes the effects of pipe heat losses and heat exchangers. This information is used as input to a design method program to estimate the long term performance of the system.

The test method may be used to calculate the effectiveness of in-tank heat exchangers and the flow rate of collector circulating fluids. These values may be used to diagnose problems in system operation and evaluate the effects of system modifications.

TABLE OF CONTENTS

LIST OF TABLES

LIST OF FIGURES

NOMEMCLATURE

A_c	Collector gross area
b_o	Collector incident angle modifier
C_p	Specific heat
Δt	Time period of integration
η	Collector efficiency
η_{del}	Efficiency of auxiliary heater
ϵ_{int}	Effectiveness of internal heat exchanger
ϵ_{ext}	Effectiveness of external heat exchanger
F_r	Collector heat removal factor
F_r'	Collector heat removal factor modified for heat exchanger
f	Solar fraction
f'	Another solar fraction
f"	Still another solar fraction
F	Long term average annual solar fraction
Ht	Daily average monthly radiation incident on a tilted surface
I_r	Effective incident radiation
I_t	Tilted surface insolation
$I_{t,c}$	Tilted surface critical insolation level
L	Thermal load on system
M	Monthy water usage

$\dot{m}_{load}$	Mass flow rate of water to load
$\dot{m}_{coll}$	Collector fluid flowrate
$(\dot{m}C_p)_c$	Collector loop capacitance rate
$\dot{m}$	Mass flow rate
N	Number of days in month
$\bar{\phi}$	Monthly average utilizability
ϕ	Utilizability
$\dot{q}_{loss}$	Rate of heat loss
$\dot{q}_{solar}$	Rate of solar input
$\dot{q}_{useful}$	Rate of useful energy gain
$\dot{q}_{load}$	Rate of energy delivery to load
q_{purch}	Rate of purchased energy use
$\dot{q}_{aux}$	Rate of auxiliary energy delivery
Q_{useful}	Integrated useful gain of collector loop delivered to storage
Q_{aux}	Integrated auxiliary energy delivered to system
Q_{conv}	Integrated auxiliary energy used by conventional system
Q_{load}	Integrated load energy removed from system
Q_{loss}	Integrated energy loss from system
$Q_{operating}$	Integrated operating energy used by system fans, pumps, controllers, etc.
$(\tau\alpha)$	Transmittance-absorptance product of cover-absorber system

$(\tau\alpha)'$	Transmittance-absorptance product modified fu-pipe losses
$(\overline{\tau\alpha})$	Monthly average transmittance-absorptance product
$\Delta\tau$	Time interval
T_{in}	Collector loop inlet temperature
T_{amb}	Collector ambient temperature
$(\Delta T)/I$	Collector loop operating point
T_{del}	Hot water delivery temperature to load
T_{mains}	Mains water temperature
T_s	Average temperature of solar tank
T_{aux}	Auxiliary heater set temperature
T_{env}	Tank environment temperature
T_{set}	Auxiliary heater set temperature
T'_{min}	Montly average collection temperature
T_t	Monthly average storage temperature for losses
T'	Bulk average storage temperature
T	Time averaged value of T'
$(\tau\alpha)_n$	Transmittance-absorptance product at normal incidence
θ	Incident angle
U	Internal energy
U_l	Overall collector loss coefficient
U_l'	Overall collector loss coefficient modified for pipe losses

$(UA)_{solar}$	Solar (preheat) tank overall area-conductance product
$(UA)_{auxiliary}$	Auxiliary tank overall area-conductance product
$(UA)_o$	Area-conductance product of collector outlet piping
$(UA)_i$	Area-conductance product of collector inlet piping
Y	Dimensionless collector gain

Chapter 1

Survey of Solar Domestic Hot Water Systems

1.A Introduction

This thesis describes the development, construction and use of a device for testing the performance of solar domestic hot water system *in situ* over a short period of time.

With the increasing use of solar domestic water heating comes a need for diagnostic techniques which may be used on installed sytems. Diagnostic techniques have two areas of application: 1) verification of system operation, both overall and on a component-by-component basis, and 2) prediction of long-term performance.

Verification of installed SDHW system performance is difficult without a means to measure the large number of environmental and use factors which affect sytem operation. The methods described and demonstrated in the following chapters provide a means of verifying proper system operation and identifying problem areas.

Long term performance predictions based on manufacturer's data have a high degree of uncertainty due to variations in installations and other factors.

If the actual characteristics of installed systems are used in long term analyses, the quality and accuracy of performance predictions will be improved.

This thesis is divided into five chapters and supporting appendices.

Chapter 1 describes solar domestic hot water systems and surveys existing test methods.

Chapter 2 presents an in situ test method.

Chapter 3 describes the data acquisition system used to implement the test method developed in Chapter 2.

Chapter 4 contains the results of system tests.

Chapter 5 discusses improvements and extensions of the in situ testing method.

Following Chapter 5 are listings of the various software routines developed for this project.

1.B Solar Domestic Hot Water Systems: Function and Components

A solar domestic hot water system is designed to deliver heated water to a point of use. Part or all of the energy added to the water is made up from solar thermal sources. Water delivered by the system is not recirculated, and is made up by the local potable water supply.

The open system configurations and moderate delivery temperatures characteristics of SDHW systems imply that they could be an effective and useful application of solar energy.

SDHW system components fall into five functional groups performing the tasks of collection, storage, delivery, auxiliary supply and control. (The storage and auxiliary supply functions may be absent from a system.)

1.B.1 Collection

The collection sub-system converts sunlight into thermal energy and provides a coupling to the rest of the system. Collectors may be classified, among other ways [1], with regard to their thermal storage capacity into those with low storage capacity and those with (intentionally) high thermal storage capacity. The

latter type integrates the storage function with energy collection, resulting in a simplified system.

Systems with separate collector and storage units may be classified by the method used to transport thermal energy to storage. There are two considerations here: the fluid used and the driving force for circulating it.

Heat transfer fluids may be divided into potable and non-potable media. Non-potable fluids require a further heat exchange step in which heat is transferred to the storage from the heat transfer fluid. This heat exchange step may occur through an immersed coil or jacketed tank, with the storage side fluid driven by natural convection. This type of heat transfer characterizes an indirect system. If the last heat exchange step occurs outside the storage (i.e., an external heat exchanger) the system is a direct type. A system using potable water in the collectors is a special case of the direct system.

Either of these systems, direct or indirect, may use one of two methods to circulate the collector fluid. One method, the thermosiphon, uses the density differences occuring in the collector loop to provide a hydraulic head. A thermosyphon system does not need a

circulating pump or a pump controller in the collector loop, since flow begins when the outlet temperature is high enough to displace colder water in the loop. The system must be laid out so that part of the collector is placed at a lower level than the storage and provisions must be made to guard against backflow and freezing. Thermosyphon systems see wide use throughout the world but are somewhat less popular in the U.S., where the collector-below-storage requirement has made them difficult to integrate with the structure and plumbing of conventional homes. The difficulty of incorporating freeze protection in thermosyphon systems has also inhibited their acceptance in the U.S.

1.B.2 Storage

Storage systems generally consist of a fixed volume of potable water held in one or more tanks. Variations on this scheme (i.e., other media such as rock beds and phase change materials) are common in SDHW systems which are part of a space conditioning system. These wil not be considered here.

Storage until temperatures are usually well above those of the surroundings. Heat loss from storage must be controlled by adequate insulation. Systems which integrate collection and storage functions have the

more difficult problem in controlling storage losses. Solutions involving movable insulated coverings have been used, among others.

1.B.3 Auxiliary Suppy

Storage and auxiliary supply functions may be integrated in the same unit. In order to maintain high efficiency, water heated by the auxiliary should not be allowed to enter the collector loop. This is easily accomplished in the case of electric auxiliaries. Auxiliary energy may also be supplied through an in-tank heat exchanger. The energy source in this case may be a boiler, heat pump or waste heat from another process. Direct fired auxiliaries are seldom integrated with the primary storage and are commonly applied to a separate tank or heat exchange unit.

1.B.4 Controls

Controls fall into several categories. By function these include: collector circulation, freeze protection, overheating protection (collector and/or storage), auxiliary supply and discharge temperature control (tempering).

Collector circulation control is usually accomplished by using a differential controller, a

device which measures the temperature difference between the collector plate (near the outlet) and the lower part of the storage tank. If the difference exceeds the turn-on differential, the pump is energized. The turn-off differential is set lower than the turn-on point so that the controller will be stable.

The simple on-off control scheme may be modified to allow variations in the pump flow proportional to the collector outlet to tank temperature difference. In this scheme the collector flowrate is low for low temperature differences and high for high temperature difference.

Control strategies (excluding anti-freeze filled collector loops) to prevent freezing fall into two classes: freeze-point circulation and collector draining. Freeze point circulation is used only when freezing conditions are not normally encountered. This technique involves monitoring plate or ambient temperatures and activiting the pump when the freezing point is approached. Energy is wasted in the process, making this more of an emergency protection method than a normal operating procedure. Also, this technique will not work during long periods of freezing weather

as storage temperatures will eventually approach the freezing point and the collector will freeze anyway.

A more practical anti-freeze control strategy for cold climates is the drain-down or drain-back technique. When this technique is used the collectors are filled with water only when solar energy is available. When energy collection ceases, the collectors are drained either into the storage tank, a special 'drain-back' reservior or to waste. Care must be taken during system installation to ensure that the collectors and exposed piping fill and drain completely.

Overtemperature control is needed in both the collector loop and in storage. Pressure-temperature relief valves are required by plumbing codes for both tanks and closed circulating loops. Circulator controllers often include overtemperature cutout circuits to ensure that the storage temperature does not exceed a set value (approximately 80 C or 180 F).

Collector loop overtemperature control is eased by the fact that many of the flat plate collectors used in SDHW systems do not have an equilibrium temperature high enough to boil the circulating fluid. However, glycol-based heat transfer fluids tend to degrade at

high temperatures and produce acid byproducts. A few collectors have been constructed with a venting feature to alleviate overheating.

Auxiliary controllers attempt to maintain some minimum temperature at the point of water use and usually of the on-off type. The controller senses a temperature related to the part of the tank heated by the auxiliary and supplies an 'ON' signal until the temperature exceeds an upper (adjustable) setpoint. Commerically available controllers have a large amount of hysterisis, with the difference between on and off setpoints often exceeding 10 C. This is intended to prevent unstable operation.

Discharge temperature control is provided by the so-called 'tempering' valve which mixes cold mains with heated water so that the outlet temperature does not exceed a set value. This action restricts flow out of the system under conditions of high storage temperature and is both beneficial and harmful to system performance [2].

1.B.5 Contemporary Domestic Water Heating Economics

Conventional domestic hot water systems have evolved through many years of development and experience. Users and manufactures have come to a sort

of equilibrium regarding performance and durability. Until the steep increases in the prices of conventional fuels which occured in the 1970s, energy usage had not been a major concern of manufacturers or users. However, by 1982, a gas-fired water heater which had cost about $40 per year to operate ten years earlier was costing upwards of $160 per year in Madison. Electric-fired units cost proportionally more, with the major cost rise coming earlier than that for natural gas.

The universal availability of sunlight has prompted many attempts to use it as a source of thermal energy [3]. Until fossil fuels quintupled in price during the 1970s there was little incentive to make use of solar energy on a large scale. Intensive efforts to promote the use of solar energy during the last decade have resulted in the installation of thousands of SDHW systems in the United States. The expansion and viability of the solar industry depend on the purchaser's confidence in the money saving qualities of a system that she/he buys. This confidence can be gained only through the establishment of system performance standards which may be related directly to cost savings.

Performance standards have evolved in many industries only after years of operating experience. The solar industry, on the other hand, has tried to set performance standards while still in an early stage of its evolution. The result has been a confusing proliferation of test methods and performance criteria. The following sections discuss performance indices and test methods for SDHW systems and components

1.C SDHW System and Component Performance

A SDHW system is made up of a set of individual components each of which may be considered as a separate thermal system. Performance characteristics of each system element can be defined and are essential input to simulaton and design method algorithms. The derivation of these characteristics will be discussed in this section.

The overall performance of a SDHW system depends on the interaction of its component parts under the influence of ambient conditions. System performance may be analyzed from many different viewpoints, including thermal, economic and rescource-based. Economic and rescource-based performance evaluations are predicted on system thermal performance.

1.C.1 Individual Component Performance

1.C.1.a Collectors

A solar collector gathers ambient sunlight as thermal energy which is transferred to a storage medium. An energy balance on the collector as a whole, in rate form, is:

$$\frac{dU}{dt} = \dot{q}_{solar} - \dot{q}_{loss} - \dot{q}_{useful} \qquad (1.C.1)$$

$\frac{dU}{dt}$ is the change in internal energy of the collector, $\dot{q}_{solar}$ is the solar energy incident on the collector, $\dot{q}_{loss}$ is the solar energy lost to the surroundings, $\dot{q}_{useful}$ is the energy transferred to the storage device by the collector system.

An expression for collection efficiency may be written:

$$\eta = \dot{q}_{useful}/\dot{q}_{solar} \qquad (1.C.2)$$

If the collector thermal capacity and certain other secondary effects are neglected, the classic Hottel-Whillier [4] equation may be used to express the useful gain of the collector in terms of the ambient conditions and collector characteristics:

$$\dot{q}_{useful} = A_c F_r [(\tau\alpha) I_t - U_l (T_{in} - T_{amb})] \quad (1.C.3)$$

A_c is the aperture area of the collector, F_r is the collector heat removal factor, $(\tau\alpha)$ is the transmittance -absorptance product for the cover-absorber system, I_t is the solar flux incident on the collector (referenced to the aperture area), T_{in} is the collector inlet temperature, T_{amb} is the ambient temperature in the vicinity of the collector.

This equation may be used to express collector efficiency on an instantaneous basis by dividing both sides by the factor $A_c I_t$

$$\eta = F_r(\tau\alpha) - U_l(T_{in} - T_{amb})/I_t \quad (1.C.4)$$

If the heat removal factor, transmittance-absorptance product and loss coefficient are considered constant, 1.C.4 is a linear equation relating efficiency to the collector operating point, $(T_{in}-T_{amb})/I_t$. Although this simple relationship does not exactly represent collector operation, it is adequate under most circumstances and can be modified to account for other factors. These include the angular dependence of the

transmittance-absorptance product and the temperature dependence of the heat removal factor and loss coefficient.

Standard 93-1977 of the ASHRAE [5] provides methods for testing of collectors and allows presentation of results in plots with efficiency and $(T_{in}-T_{amb})/I_t$ as axes. The standard requires testing using near-normal incidence radiation. The ratio of aperture area to gross area and the angle of incidence dependence of the transmittance-absorptance product should be determined during such a test. Test results may be presented in the form of a first or second order curve fit to the efficiency vs $\Delta T/I$ data.

A first order curve fit to ASHRAE 93-1977 test data yields an intercept of $F_t(\tau\alpha)_n$ and a slope of $-F_rU_l$. These results are valid over the range of collector operating points tested but are generally used over the entire collector operating range. The ambient windspeed also affects test results.

The normal-incidence intercept efficiency, $F_r(\tau\alpha)_n$, may be modified by a factor to account for off-normal operation. ASHRAE Standard 93-1977 defines this factor as:

$$K_{\alpha\tau} = 1-b_o(1/\cos(\theta)-1) \qquad (1.C.5)$$

$K_{\alpha\tau}$ is the ratio of the transmittance-absorptance product at normal incidence to that at incident angle θ. The constant b_o is the slope of the line which results when $K_{\alpha\tau}$ is plotted vs the transformed angle $(1/\cos(\theta)-1)$. Typical values of b_o range from -0.05 to +0.2.

The effect of heat exchangers and pipe or duct heat losses may be included when evaluating collector loop performance. DeWinter [6] has presented a method of modifying the collector heat removal factor to account for the presence of a constant-effectiveness heat exchanger. Duffie and Beckman [1] present an algorithm for including the effect of heat losses from piping or ductwork exposed to ambient conditions.

1.C.1.b. Storage Units

Thermal storage in all SDHW systems considered in this paper is in the form of hot potable water. This is contained in one or two tanks and may also include an auxiliary heat source. An energy balance on the storage is of the form:

$$\frac{dU}{dt} = \dot{q}_{useful} - \dot{q}_{load} - \dot{q}_{loss} + \dot{q}_{aux} \qquad (1.C.6)$$

$\frac{dU}{dt}$ is the change in internal energy of the storage, $\dot{q}_{useful}$ is the useful gain of the collector loop, $\dot{q}_{load}$ is the energy lost to the environment, and $\dot{q}_{aux}$ is energy supplied to the storage from the auxiliary heat source.

The internal energy term in Equation 1.C.6 represents the change in internal energy of all storage units in the system, including that heated by auxiliary.

Energy delivered to the load as hot water may be expressed:

$$\dot{q}_{load} = \dot{m}\, C_p (T_{del} - T_{mains}) \qquad (1.C.7)$$

$\dot{m}$ is the load flow rate, C_p is the load fluid (water) heat capacity, T_{del} is the delivery temperature measured at the point of use, and T_{mains} is the make-up water temperature.

Losses from the storage system are proportional to the storage to environment temperature difference. To simplify the analysis, it is convenient to divide the storage into two fully-mixed units, each at its own temperature and having its own loss coefficient-area

product. The solar heated tank (or portion of a single tank below the auxiliary thermostat sensor) is considered to be at a temperature T_s. The auxiliary tank (or auxiliary heated protion of a single tank) is assumed to be at the thermostat set temperature or above. This temperature is designated T_{aux}. Overall heat losses are then:

$$\dot{q}_{loss} = (UA)_{solar} (T_s - T_{env}) + (UA)_{aux} (T_{aux} - T_{env}) \qquad (1.C.8)$$

$(UA)_{solar}$ is the solar tank's overall area-conductance product, T_s is an average temperature of stored water, T_{aux} is the auxiliary thermostat set temperature, $(UA)_{aux}$ is the auxiliary tank's area-conductance product and T_{env} is an appropriate ambient temperature. The (UA) products in this equation represent a proportionality constant between heat losses and average temperature difference. Calculations of (UA) values based on tank dimensions and insulation properties are often inaccurate. Experimental values of (UA) are more reliable albeit more difficult to obtain.

1.C.1.c Auxiliary Devices

Most SDHW systems include some kind of auxiliary heater. The most common type is a conventional water heater connected in series with the solar storage (i.e., a two-tank system). Heating elements (electric) are sometimes included in the upper portion of the solar storage tank, resulting in a single tank system and some performance advantages [2]. A third type of auxiliary includes little or no storage capacity and heats water on a single pass through it.

Auxiliary devices use energy from an outside source, usually purchased, to heat water from the solar tank temperature, T_s , to the set temperature T_{aux}. Some tank losses are also made up from the purchased source and have been included in the overall system loss term, Equation 1.C.8. The purchased energy is:

$$\dot{q}_{purch} = \frac{\dot{q}_{aux}}{\eta_{del}} \qquad (1.C.9)$$

η_{del} is conversion efficiency of the heat source, and $\dot{q}_{aux}$ is the energy needed to heat the load flow from T_s and T_{aux} plus the energy needed to make up heat losses from the auxiliary tank.

The most common sources of auxiliary heat are

fuels (natural gas and fuel oil) and electricity. A value of 60% conversion efficiency is common for fuel-fired conventional water heaters, while electric units operate at nearly 100%. The need for high-temperature venting of combusion products is the main factor causing the low efficiency of fuel-fired units.

1.C.1.d Circulator Controllers

Circulator controllers are usually designed to maximize the amount of useful energy collected. This is accomplished by maintaining collector flow only when collector outlet temperature is greater than storage temperature. Flow stops when the collector outlet to storage difference becomes less than some preset value. Flow restarts only when the temperature difference is again greater than another, larger, value. The ratio of turn-on to turn-off temperature difference must be above a minimum value to prevent instability, as shown by Duffie and Beckman [1].

The control described above is the simple 'on-off' type. Another type of controller is the proportional type, which adjusts flow in direct proportion to the storage-to-collector temperature difference.

The thermal effects of control strategies have been explored in several studies [7] and will not be

discussed further here.

1.C.2 Overall System Performance

Overall system performance is determined by the interaction of ambient conditions, individual component performance and water usage.

If the storage energy balance, Equation 1.C.6, is integrated over a long period (i.e., weeks or months), the integral of the dU/dt term becomes very small compared with the other terms and the result may be expressed:

$$Q_{useful} + Q_{aux} = Q_{load} + Q_{loss} \qquad (1.C.10)$$

Q_{useful} is the net collector output delivered to the storage unit over the time period. Q_{aux} is the net auxiliary source energy added to the water, and Q_{load} is the net energy delivered to the load as hot water (the integral of Equation 1.C.7).

The solar fraction, a useful system performance index, may be defined as:

$$f = (Q_{load} - Q_{aux})/Q_{load} \qquad (1.C.11)$$

This index relates energy delivered as hot water to

auxiliary energy used. It is possible to define other 'solar fractions' depending on the exact definition of the load and auxiliary terms in the above expression.

The auxiliary term may include energy required to operate pumps, fans and control equipment. This is correct insofar as economic (either monetary- or resource-based) analysis is concerned. However, little of this energy appears as heat gained or lost by water in the system. This leads to the definition of an additional solar fraction, f':

$$f' = 1 - (Q_{aux} + Q_{operating})/Q_{load} \qquad (1.C.12)$$

$Q_{operating}$ is the total energy used by system controls and mechanical equipment.

Another solar fraction may be defined by including losses from auxiliary-heated tanks or portions of tanks in the load term. This is not strictly correct thermodynamically, as some of the auxiliary tank losses are made up by the auxiliary element. This inclusion is a convenience for dividing the system into solar and auxiliary portions for design method analysis such as f-Chart [13]. Under these circumstances the solar fraction is:

$$f'' = 1 - (Q_{aux})/(Q_{load} + Q_{loss\text{-}aux}) \qquad (1.C.13)$$

The load term in the above expressions is dependent on the overall system performance in that the solar tank may be heated above the auxiliary set temperature. Since Equation 1.C.7 defines Q_{load} as energy delivered to the point of use as hot water, a higher-performing system will show a higher load if T_{del} is greater than T_{aux}.

Since many systems are installed with an outlet mixing valve which reduces the outlet temperature to a set value, it is convenient to consider the system delivery temperature to be the auxiliary set temperature. This prevents confusion over the definition of the system load when calculating the solar fraction.

The amount of purchased energy required by the system depends on the efficiency of the auxiliary unit. The purchased energy required by a system can be calculated using Equation 1.C.12 and considering the auxiliary device to have a constant conversion efficiency:

$$Q_{purch} = \frac{Q_{load}\ (1-f')}{\eta_{del}} \qquad (1.C.14)$$

Q_{purch} is the total purchased energy requirement of the system.

Since $Q_{operating}$ is usually very small compared with Q_{aux}, Equation 1.C.14 will give nearly the same result if f were substituted for f'.

1.D Prediction of System Performance

Predictions of long term average system performance are based on a multitude of assumptions. These assumptions fall into three interacting categories: meteorological input, component representation and analytical method.

1.D.1 Meteorological Input

The meteorological data base used in the prediction of long term performance may vary in detail from month-by-month values of solar radiation incident on a horizontal surface and ambient temperature to hour-by-hour values of direct normal and diffuse radiation, wind speed, wet-bulb and dry bulb temperatures. The average values are chosen so as to represent two aspects of weather: the long term average values and the variability of the data about

the long term average.

Simplified (monthly average) data bases contain only a limited amount of data concerning weather variability. An analytical technique that uses a database of this type must address this problem. The early work of Liu and Jordan [8]

explored the relationship between cloudiness index and variability in available sunlight. This factor has been built in to the $\bar{\phi}$, f-Chart method developed by Klein and Beckman [10].

Detailed data bases developed from long term observations contain extensive information regarding weather variability. Studies of the Typical Meteorlogical Year data base [11] have shown it to resemble the long term data from which it was selected.

1.D.2 Component Representation

Component representation depends, to a large extent, on the analytical method being used. Hour-by-hour simulation lends itself well to detailed component models while other methods may include built-in assumptions about component behavior.

Solar collectors are commonly represented by paramters derived from tests conducted in accordance with ASHRAE Standard 93-1977, as discussed in the

previous section.

Detailed simulations of a system may use more complex collector representations. However, models of this type depend on knowledge of collector dimensions and materials properties as well as employing empirical heat-transfer correlations. The collector represented in this way may or may not resemble the actual unit installed in the field.

Other system components may be represented in greater or lesser detail as well. These include tanks, piping and controls. Tank heat loss data based on tests are sometimes, but not often, available. Piping length and insulation quality vary greatly from one installation to another. Controller selection and adjustment are usually based on availability and convenience rather than thermal criteria.

1.D.3 Analytical Method

Two distinct analytical methods are available for predicting system performance. One method relies on detailed simulation of all system components and inputs on an hour-by-hour basis. The simulation is carried out over a year of operation using historical meteorological data and the results are taken to be representative of long term system performance. This

technique suffers from two problems. First, the system must be represented in sufficient detail that major performance factors are included. This requires knowledge of dimensions and physical properties of system components, knowledge which may not be available to the simulator. Second, detailed simulation is computationally intensive and requires a large data base. Such computation and data base maintainence is feasible only on larger computers, resulting in a high cost per run.

Another approach to performance prediction is the so-called design method. This approach was pioneered by Liu and Jordan [12]. Klein, Beckman and Duffie later developed the f-Chart method [3] based on simulations of representative systems. Design methods have proliferated since this early work and are now in wide use. Design methods have the advantages of smaller data base and computational requirements than the simulation methods outlined above. Two design methods are of particular interest here: f-Chart and $\overline{\phi}$, f-Chart.

The f-Chart method is based on a large number of monthly simulations. The method predicts the long term monthly average solar fraction and requires site-

specific monthly avearge values of horizontal surface total insolation and ambient temperature. Minimum system data needed to use the f-Chart method include collector area and orientation, first order coefficients of ASHRAE 93-1977 test results, cover characteristics, storage capacity, mains temperature, auxiliary set temperature and daily usage. Other system variables such as pipe insulation, collector loop heat exchangers and second tank losses may be accounted for by modifications to input values. The f-Chart method has been shown to be in substantial agreement with long term test results [14].

The $\bar{\phi}$, f-Chart method also developed by Klein and Beckman [10, 15] has been applied to a wide range of solar thermal systems. This method relies on the concept of monthly average solar utilizability, a system statistic which may be calculated form long term weather data and system parameters. Klein and others [16] have developed correlations of utilizability in terms of critical level, cloudiness index and system geometry.

Utilizability is the fraction of incident radiation that can be converted to useful heat by a collector with $F_r(\tau\alpha) = 1$ and operating at a fixed

inlet temperature. For a particular collector, the critical radiation level is defined as the intensity of incident radiation required to produce useful output for given ambient and inlet temperatures. This may be expressed as:

$$I_{t,c} = \frac{F_r U_l (T_{in} - T_{amb})}{F_r(\tau\alpha)} \qquad (1.D.1)$$

On a monthly basis, the critical level may be calculated using representative values of T_{in}, T_{amb} and $(\tau\alpha)$. This leads to the definition of monthly average utilizability, the fraction of daily average monthly radiation incident on the collector which is above the critical level. This may be expressed as:

$$\bar{\phi} = \sum_{\text{days}} \sum_{\text{hours}} \frac{(I_t - I_{t,c})^+}{\bar{H}_t N} \qquad (1.D.2)$$

The '+'sign in the numerator indicates that only the positive values are to be summed. $\bar{H}_t$ is the daily average monthly radiation incident on the collector, N is the number of days in the month, I_t is the hourly radiation and $I_{t,c}$ is the monthly avearge critical level.

The maximum monthly average daily useful energy

production of a solar collector can be calculated as:

$$Q_u = A_c F_r (\overline{\tau\alpha})\ H_t \bar{\phi} \qquad (1.D.3)$$

1.D.5 $\bar{\phi}$, f-Chart for Solar DHW Systems

The utilizability concept has been incorporated into the $\bar{\phi}$, f-Chart design method. The implementation of this design method of interest here is that presented by Braun, Klein and Pearson [17]. The method uses correlations for monthly-average hourly values of utilizability developed by Clark [16].

The $\bar{\phi}$, f-Chart method may be applied to DHW systems by considering a monthly energy balance on the system:

$$Q_u - Q_{loss} - Q_{load} = 0 \qquad (1.D.4)$$

Q_u is the collector loop again, Q_{loss} is the energy lost from storage and Q_{load} is the energy supplied to the load. Equation 1.D.4 assumes that the monthly change in internal energy of the storage is small.

The collector loop gain is calculated as:

$$Q_u = Q_{u-max} - a(e^{bf}-1)(1-e^{cx})e^{dz_L} \qquad (1.D.5)$$

Where:

$$Q_{u-max} = A_c F_r' (\tau\alpha)' \bar{\phi}_{max} (T'_{min}) H_t N \qquad (1.D.6)$$

$a = 0.015 (C_s/350 kJ/m^2\text{-}C)^{-0.76}$

(C_s is the thermal capacitance of storage)

$b = 3.85$

$c = -0.15$

$X = eA_x F_r' U_1' (100C) \Delta t/L$

$d = -1.959$

$Z = \dfrac{L}{M\ C_p (100C)}$

The monthly water usage, M, is adjusted to include the effects of heat losses from the auxiliary storage tank and is calculated as:

$$M = \int_{\Delta t} \dot{m}_{load}\ dt + \frac{(UA)_{aux}\ (T_{aux} - T_{env})\Delta t}{C_p (T_{aux} - T_{mains})} \qquad (1.D.7)$$

$\dot{m}_{load}$ is the flow to the load, $(UA)_{aux}$ is the area-conductance product of auxiliary storage, T_{aux} is the auxiliary set temperature. T_{env} is the storage tank's environment temperature, Δt is the time period, C_p is the specific heat of water and T_{mains} is the system's make up water supply temperature.

The system load, L, is defined as:

$$L = M\ C_p\ (T_{aux}-T_{mains}) \qquad (1.D.8)$$

The monthly average delivery temperature, T'_{min} is used in calculating $\overline{\phi}_{max}$.

The monthly average storage temperature for losses is defined as:

$$T_t = T'_{min} + g(e^{kf}-1)\ e^{hz} \qquad (1.D.10)$$

where:

$g = (0.214C)\ C_s/350kJ/m^2\text{-}C)^{-.704}$

$h = -4.002$

$k = 4.702$

Storage losses are calculated as:

$$Q_{loss} = (UA)_{solar}(T_t-T_{env})\Delta t$$

where:

$(UA)_{solar}$ is the area-conductance product for the solar storage tank and T_{env} is the temperature of the storage tank's environment.

The solar fraction for the system is defined:

$$f = \frac{Q_u-Q_{loss}}{L} \qquad (1.D.11)$$

Application of this method to a particular system involves the iterative solution of Equations 1.D.5, 1.D.9, 1.D.10 and 1.D.11 for the average collection and delivery temperature, T'_{min}. This tedious procedure has been implemented in the computer program FCHART 4.1 [15] which was used to generate the system performance estimates contained in Chapter 4.

1.E Survey of Solar Domestic Hot Water System Testing

Solar domestic hot water system tests can be classifed by the conditions and duration of the test, with systems tested under laboratory or field conditions for short or long periods. For all testing situations, there is great variation in the detail and resolution of data gathered.

Laboratory tests are undertaken on specially-constructed systems which are operated under controlled conditions. Energy input to laboratory systems may be from ambient sources, i.e. 'ordinary' sunshine, a solar simulator or from a conventional energy source such as an electric resistance heater. Laboratory tests have been undertaken by the US National Bureau of Standards [18], the Florida Solar Energy Center [19] and others.

.Field tests involve systems in actual use. The systems tested in the field are often 'generic' types

installed by local contractors in accordance with accepted industry practice, as in the Wisconsin Power and Light [20], the Northeast Solar Energy Center [21] and Penn State [22] programs. A few specially-constructed 'demonstration' systems have been tested in the field. The results of these tests have been reported by the National Solar Data Network [23].

1.E.1 Long Term Testing

Long term system testing covers one or more continuous years of operation and can range in detail from regional surveys of systems in the field [22,20,21] to elaborage networks of data acquisition systems [23]. The NBS has carried out long term testing of systems under laboratory conditions over a period of two years, gathering highly detailed data on system operation.

As long term testing is feasible only under outdoor conditions, constraints of climate and the variability of weather become important considerations when interpreting results. The timing and duration of water usage is also an important factor in long term tests. These factors may be easily controlled under laboratory conditions, as in the NBS tests. Under field conditions, however, wide variations in timing

and volume of hot water usage are common. Analysis of long term field test data must take this into account.

1.E.2 Short Term Testing

Short term tests cover periods under a year and may range in duration from a single day to several months and may be undertaken either under laboratory or field conditions.

Short term tests have two different goals: performance rating and performance verification. Most of the short term testing work that has been carried out in recent years has been directed toward developing rating procedures.

Rating tests are designed to provide information on the performance of different systems under similar conditions. Rating tests implicitly assume that the system under test is operating properly and is a representative sample of the system as it would be installed in the field.

Performance verification tests, on the other hand, are designed to provide diagnostic information and performance data which may be compared with design values for the particular system undet test. This type of test would normally be done only on field installed systems.

Two groups, the Florida Solar Energy Center (FSEC) and the National Bureau of Standards (NBS), have been active in developing rating type tests. The FSEC [19] has developed a rating procedure based on a single day outdoor test and analytical modeling. The system under test is operated side-by-side with a 'baseline' system of known performance. The ratio of test system to 'baseline' system performance is called the relative solar rating. Long term annual performance of the tested system would be determined from the relative solar rating, a correlation procedure based on computer simulations and the long-term performance of the baseline system. This procedure is reported to be successful when applied to single tank direct systems in sunny climates but less so in a cold climate.

A test procedure has been developed which uses an indoor solar simulator to irradiate the solar panels of the system under test. The energy input is varied over the day according to a pattern specified by an industry rating organization. Energy is withdrawn from the system at prescribed intervals. Testing is continued until two successive days of identical performance are obtained. This procedure has many advantages including repeatability, independence from outdoor conditions and

independence from correlations or simulation codes. However, the limited availability and capacity of solar simulators, as well as the need to re-test each variant of a system, make this an uneconomical test method. This procedure is incorporated in the American Society of Heating Refrigeration and Air Conditioning Engineers (ASHRAE) Standard 95-1981, "Methods of Testing to Determine the Thermal Performance of Solar Domestic Hot Water System", adopted by the American National Standards Institute (ANSI) in 1981.

A. H. Fanney [24] at the National Bureau of Standards has developed a testing procedure which uses a conventional heat source such as an electric resistance heater to replace the solar input to a SDHW system. A variation of this procedure have been incorporated in ASHRAE Standard 95-1981. In this test the heat source is placed in the collector loop either upstream or downstream of the collector. Power input to the system is varied so that the collector-heat source combination supplies the same net input as an irradiated array. Excellent agreement between this procedure and long term laboratory tests has been reported.

ASHRAE Standard 95-1981 does not specify test

conditions. These are left to the industry rating organizations. Two organizations have developed test conditions as this time. The Solar Rating and Certification Corporation (SRCC) and the Air-conditioning and Refrigeration Institute (ARI) have developed different standard data bases to represent test conditions. Tests based on ASHRAE 95-1981 may be used for rating purposes only and cannot provide any prediction of long term performance.

A testing method aimed at providing both rating and long term performance information was developed at NBS by Klein and Fanney [25]. The technique involves two tests performed in accordance with ASHRAE 95-1981. In one test the system is operated so that it provides a low (less than 20%) solar fraction, with a high solar fraction (more than 60%) provided in the second test. The first test can be performed with zero solar input if the system can supply all the auxiliary energy required to meet the load under these conditions. For each test the daily values of the system solar fraction and utilizability are calculated using the expressions.

$$f = 1 - Q_{aux}/Q_{load} \qquad (1.E.1)$$

$$\phi Y = \phi \; F_r(\tau\alpha)H_t/Q_{load} \qquad (1.E.2)$$

$$\phi = \frac{\Sigma(I_t - I_{t,c})^+}{\Sigma I_t} \qquad (1.E.3)$$

$$I_{t,c} = \frac{F_r U_l}{F_r(\tau\alpha)} \; (T_s - T_{amb}) \qquad (1.E.4)$$

f is the daily solar fraction, Q_{aux} is energy used by the auxiliary heater, Q_{load} is energy removed from the system as hot water, H_t is total daily solar radiation incident on the collector array, I_t is instantaneous array irradiance, T_s is a representative storage temperature and T_{amb} is the ambient temperature.

Klein and Fanney observed that if ϕY and f from several tests of the same system are plotted on the same axes, a straight line results if the representative system temperature is chosen correctly. The correct choice for T_s was found to be the average temperature of water in the solar heated portion of the storage tank during the collection period.

The results of the short term tests may be extrapolated to annual performance estimates by using an iterative procedure. The procedure involves

calculating monthly average values of Y, T_s, I_c and ϕ. The product ϕY product is then used to obtain a monthly average value of f using the linear relationship between ϕY and f generated in the short-term tests. Since T_s depends on f, the procedure must be repeated until the results from one iteration to the next are in substantial agreement.

Monthly average values of f calculated using the above procedure are averaged over the year using the expression:

$$F = \frac{\Sigma f\ Q_{load}}{\Sigma\ Q_{load}} \qquad (1.E.5)$$

F is the long term annual average solar fraction and Q_{laod} is the long term average monthly system load. This method has been shown to be in good agreement with test results.

1.F Desirability and Limitations of Short Term SDHW Testing

Designers, manufacturers, installers and owners of SDHW systems are today faced with a serious dilemma. The economic viability of a solar installation depends on its long term thermal performance, but this performance depends both on the system components and

on the variability of ambient conditions. Several years of operating history are needed to draw firm conclusions about the real energy savings of a system. However, decisions on systems must be made now, not in the future. The only way out of this is the development of standardized rating procedures. These procedures must be based on short term tests or risk imposing one-year or more lead times on solar manufacturers.

Once short term testing has been established as the preferable method, test goals must be chosen. Two performance figures are commonly used. The first is a relative system rating for operation under standard conditions such as ASHRAE 95-1981 as implemented by SEIA and SRCC. The other is expected long term average system performance for a particular site. The latter figure is more desirable in that it provides information which may be used to evaluate system economics. Relative ratings, however, are easier to generate and have the distinct advantage of being derived directly from experiment rather than the extrapolation based on theory needed to develop long term performance estimates from system parameters or short term tests.

The short term tests developed by NBS and FSEC are strictly whole-system tests. Any change in the system necessitates a re-test of the entire unit. With all the possible variations in collector area, tank volume and controls available, the time and cost of testing one manufacturer's line of systems would be enormous. The test method proposed by Klein and Fanney and outlined in the previous section allows variation of some system parameters, notably collector area, in calculating long term performance.

There is a clear need for a test method which lies somewhere between the detailed single system tests of NBS and FSEC and the long term area-wide surveys of Penn State, NESEC and others. Such a testing method would allow testing of systems in situ with a level of detail sufficient to provide for prediction of long term performance. The remainder of this thesis will describe the development of such a methodology and its implementation.

Chapter 2

Short Term Test Theory

An ideal short term in situ test would provide an estimate of long term system performance in the shortest possible testing period without upsetting operation of the system. There are three different points to be considered here: performance estimation, test duration and system operation during the test.

2.A.1 Test Output Requirements

Long term performance estimates may be obtained by using one of the design methods outlined in the previous section. These methods require data on collector performance, orientation, area, flowrate, tank and piping conductance-area products, heat exchanger effectiveness, mains temperature, auxiliary set temperature and daily water usage. Also needed are site-specific data on long term monthly average insolation and ambient termperatures.

Of these data, only a few may be easily determined. Collector area and orientation may be readily measured. Mains and auxiliary set temperatures may also be measured but may have large short and long term variations. Little else about the system may be measured directly.

Some system parameters may be measured indirectly, as will be seen below. These include collector performance, flowrate, tank area-conductance product and heat exchanger effectiveness.

Some system parameters must be inferred from other sources. This includes daily water usage and pipe heat loss. Variations in daily water usage may be considerable and will have a drastic effect on day-to-day performance. Estimates of long term daily average usage have been provided by some studies [26, 20] but data are sparse in this area.

Although pipe runs may be measured and data on insulation conductances are available, the actual value of pipe insulation is difficult to estimate. The same holds true for tank area-conductance products.

Site-specific data on long term average insolation and ambient temperatures are available from several sources. The most extensive data base in this area is contained in the US government publication "Input Data for Solar Systems" [27] and contains data for more than 150 locations in North America. Another data base is the Typical Meteorological Year [11] data developed by several groups working under the auspices of the US Department of Energy. This data base consists of

hourly observations primarily taken from historical records and enhanced by modeling efforts. Although the TMY data are hourly values, averages derived from the data can be expected to be near the long term average for the site.

2.A.2 Test Duration

An ideal test method would require a one-time test of very short duration, i.e., a few minutes. Simple yes-no tests of control elements may be done in this time frame but all other system components require a longer period. As will be seen later, the best that can be expected is a test that requires a 72 hour period to complete. At worst, weeks of testing may be required to gather sufficient data for reliable prediction of system thermal performance.

2.A.3 System Operation During Testing

Since this testing methodology is aimed at on-site evaluation of installed systems an important consideration is the continued operation of the system during the testing period. This is possible only under two conditions. First, a two-tank system with separate solar and auxiliary tanks may be operated in an auxiliary-only mode if the solar tank is bypassed. In

this case hot water is provided to users on demand without the necessity of monitoring delivered flow and temperatures. Second, if the load flowrate and temperature can be monitored continuously in with other system variables, load flow may be allowed through the solar tank. As will be seen shortly, this monitoring is not feasible given other constraints of the testing process. This creates a problem for testing single tank systems since auxiliary and solar tanks are combined in this type of layout and bypassing is impossible. The only available alternative is to use the shortest possible testing cycle during which hot water supply to the load is cut off.

2.B Testing Methodology

As outlined in the previous section, an ideal test would entail no interruption of service, require one-time measurements and would provide long term performance estimates directly. However, many compromises must be made in the development of a practical test. An examination of the system energy balance and individual component performance factors will give clues to these compromises.

2.B.1 Test Energy Balance

An energy balance on the collector and storage system was developed in section 1.C and is repeated here for clarity:

$$\frac{dU}{dt} = \dot{q}_{useful} - \dot{q}_{load} - \dot{q}_{loss} + \dot{q}_{aux} \qquad (2.B.1)$$

The components of this equation may be expanded as follows:

$$\frac{dU}{dt} = M\ C_p\ \frac{dT}{dt}$$

$$\dot{q}_{useful} = A_c F_r' [(\tau\alpha)' I_t - U_l (T_{in} - T_{amb})^+]$$

$$\dot{q}_{load} = \dot{m}_{load} C_p (T_{del} - T_{mains})$$

$$\dot{q}_{loss} = (UA)\ (T_{tank} - T_{env})$$

$$\dot{q}_{aux} = \eta_{del} (\dot{q}_{purch})$$

Where:

M	is the mass of the storage fluid
C_p	is the constant pressure specific heat of the fluid

$\frac{dT}{dt}$ is the derivative of average storage temperature with respect to time

A_c is collector aperture area

F_r' is the collector heat removal factor adjusted for heat exchanger effects

$\dot{m}_{load}$ is the load flow rate

η_{del} is the auxiliary conversion efficiency

$\dot{q}_{purch}$ is the energy delivered to the auxiliary device

This expression may be simplified by the elimination of two terms, both of which are difficult to measure. There are the load energy, $\dot{q}_{load}$, and the auxiliary energy, $\dot{q}_{aux}$.

Load energy is difficult to measure because the load mass flow is subject to the demand of system users and can vary over a wide range. Instantaneous readings of mass flow rate would require the installation of a flow meter (turbine or other type) in the delivery piping, a plumbing job outside the bounds of a short term test. In addition, load flow would remove energy from the tank, reducing its temperature and in turn reducing the spread of collector operating points on a given day. Load flow may be eliminated from the solar

tank by either shutting off the mains supply to the system or bypassing it to the auxiliary tank, if present.

Auxiliary energy, like load energy, is both difficult to measure (except electric input) and tends to introduce further variables into performance expressions. Since the auxiliary is often integrated into a separate tank from the solar storage, elimination of this term reduces the number of measurements that need to be made. In addition, instantaneous measurements of auxiliary energy usage are difficult to make when dealing with a fuel-fired device such as a natural gas fired water heater.

2.B.2 Collector Loop Performance

With the elimination of the load and auxiliary terms and substitution of the individual componenet performance expressions the energy balance equation becomes:

$$M\,C_p\,\frac{dT}{dt} = A_c F_r'[(\tau\alpha)I_t - U_l(T_{in}-T_{amb})] - (UA)(T_{tank}-T_{env}) \qquad (2.B.2)$$

$$\eta_{coll} = \frac{M\,C_p\,\frac{dT}{dt} + (UA)\,(T_{tank}-T_{env})}{A_c I_t} \qquad (2.B.3.a)$$

$$\eta_{coll} = F_r'(\tau\alpha) - \frac{U_l(T_{in}-T_{amb})}{I_t} \qquad (2.B.3.b)$$

The second form of the equation is a linear expression of collector efficiency in terms of its operating point, $(T_{in}-T_{amb})/I_t$. This holds true only in an approximate sense, since $(\tau\alpha)$ is a function of insolation incident angle, and F_r' and U_l are functions of several variables. These considerations aside for the moment, let us explore the uses of the expression derived above.

The collector efficiency equation (2.B.3.a) may be numerically integrated over some finite time interval $\Delta\tau$ resulting in an expression:

$$\eta_{coll} = \frac{M\,C_p(T'-T) + \int_{\Delta\tau}(UA)(\hat{T}-T_{env})\,dt}{A_c \int_{\Delta\tau} I_t\,dt} \qquad (2.B.4)$$

Where:

T' is the average storage temperature at the end of the time interval

T is the average storage temperature at the beginning of the interval

$\hat{T}$ is the time averaged storage temperature over the time interval

$\Delta\tau$ is the (finite) time interval of integration

I_t is the instantaneous insolation on the collector aperture.

If the time period involved is short enough (e.g., a few minutes), the collector operating point may be considered constant. Efficiency vs operating point data can then be plotted to yield an estimate of the collector loop performance. A linear regression on these data, over a wide enough range of conditions, will then yield estimates of $F_r'(\tau\alpha)$ and $F_r'U_l$. These estimates of collector loop performance are that as 'seen' by the tank and so include the effects of pipe heat losses and heat exchangers.

2.B.3. Storage Tank Losses

The area-conductance product of the storage tank may be estimated by using a similar approach. If all the terms except $\dot{q}_{loss}$ are eliminated from the right side of equation (2.B.1), the tank energy balance becomes:

$$\frac{dU}{dt} = \dot{q}_{loss} \qquad (2.B.5)$$

Expanding the q_{loss} and $\frac{dU}{dt}$ terms yields:

$$M\ C_p \frac{dT}{dt} = -\ (UA)(T-T_{env}) \qquad (.2.B.6)$$

Assuming that M C_p, (UA) and T_{env} are constant, a solution to this equation is:

$$\ln[(T-T_{env})/(T-T_{env})_o] = -\ (UA)\ (t-t_o) \qquad (2.B.7)$$

Where:

$(T-T_{env})/(T-T_{env})_o$ is the ratio of the current tank-ambient temperature difference to that at some arbitrary time zero (t_o).

$(t-t_o)$ is the elapsed time since time zero. Equation 2.B.7 is linear with a slope of -(UA) and an intercept of zero. This suggests that plot of the natural log of the temperature difference ratio vs time will allow determination of the tank area-conductance product.

2.B.4 Collector Loop Flowrate

The flowrate of fluid in the collector loop may be estimated by using an expression similar to Equation 2.B.4:

$$\dot{m}_{coll} = \frac{M\ C_p(T'-T) + \int_{\Delta T}(UA)(T-T_{env})dt}{C_p(T_{out}-T_{in})_{avg}} \qquad (2.B.8)$$

$\dot{m}_{coll}$ is the average collector fluid flowrate over the interval, $\Delta\tau$ and $(T_{out}-T_{in})_{avg}$ is the average collector loop temperature rise over the same interval.

Equation 2.B.8 may be evaluated over short periods of time during the collector operating period and the resulting values averaged to obtain an estimate of the collector loop flowrate.

2.B.5 Heat Exchanger Effectiveness

The effectiveness of internal and external heat exchangers used in a system may be estimated provided some assumptions are made about the relative magnitude of hot and cold side flowrates.

An energy balance on a heat exchanger which is perfectly insulated is of the form:

$$C_H(T_{hi}-T_{ho})=C_C(T_{ci}-T_{co}) \qquad (2.B.9)$$

C_h and C_c are the hot and cold side capacitance rates (i.e., $\dot{m}\,C_p$), T_{hi} is the most side inlet temperture, T_{ho} is the hot side outlet temperature, T_{ci} and T_{co} are the corresponding cold side outlet temperatures.

The maximum rate of heat transfer is:

$$\dot{q}_{max} = C_{min}(T_{hi} - T_{Ci}) \qquad (2.B.10)$$

C_{min} is the minimum of C_h and C_c.

The actual rate of the heat transfer is given by Equation 2.B.9. The ratio of actual heat transfer to maximum possible is the effectiveness of the heat exchanger. For an immersed coil as used in some types of SDHW tanks, the collector loop capacitance rate may be assumed to be C_{min} and the effectiveness may be calculated:

$$\varepsilon_{int} = \frac{T_{hi} - T_{ho}}{T_{hi} - T_c} \qquad (2.B.11)$$

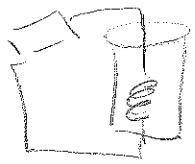

T_c is the fluid temperature on the cold side of the unit and is equal to the average tank temperature in the region of the heat exchanger.

Equation 2.B.11 may be evaluated over short periods of time during the collector operating period and the resulting values averaged to obtain an estimate of the heat exchanger effectiveness.

A similiar procedure could be followed for evaluating external heat exchangers. If the collector side capacitance rate is assumed to be the minimum, the effectiveness would be:

$$\varepsilon_{ext} = \frac{T_{hi}-T_{ho}}{T_{hi}-T_{ci}} \qquad (2.B.12)$$

If the minimum capacitance rate was on the tank side, the effectiveness would be:

$$\varepsilon_{ext} = \frac{T_{co}-T_{ci}}{T_{hi}-T_{ci}} \qquad (2.B.13)$$

2.C Short Term Test Cycle

This section will outline a short term in situ cycle which will provide data to calculate the system parameters discussed in section 2.B. The test cycle may be broken into four parts and, given ideal conditions, may be accomplished in a 72-hour period. The four parts of the test cycle are:

1) Set up data acquisition system, obtain system dimensions and other directly measurable data.

2) Assuming the storage tank is at a temperature well above its environment, shut off all external piping and heat sources. Bypass make-up water to auxiliary tank in two tank systems. Monitor average storage tank and environment temperatures for 48 hours

storage tank and environment temperatures for 48 hours or longer. These data may be used in conjunction with Equation 2.B.7 to to estimate tank (UA) product.

3) Starting with the storage tank at an average temperature of about 25-30 C, monitor system operation over one or more sunny days, gathering the data necessary to calculate component performance as outlined in section 2.B.

4) Using the data outlined in 1), 2) and 3), above, and one of the design methods outlined in section 1.D, estimate long term system performance.

This test cycle may be accomplished in 72 hours if weather and data acquisition hardware cooperate fully. Some special conditions must be met for this to hold. First, a sunny day with little water use must preceed the actual day of the test so that the 'cool-off' test (number 2 above) will yield reliable data. Second, most of the test day must be clear and sunny.

In order to better understand the test cycle and to estimate the effects of measurement errors, the following section will describe the development of a simple computer simulation of part of this test.

2.D. Computer Simulation of Test Cycle

To demonstrate the feasibility of the testing

methodology outlined in the previous section, a simulation of a simple SDHW system was developed using the TRNSYS [29] simulation program. The simulation was run at short (1/10 hour) timesteps and was set up to generate a file containing timestep-by-timestep values of tank temperature, ambient temperature, solar radiation and pump status. This file was subsequently transmitted to a microcomputer which was used to develop a data reduction program based on the equations in section 2.B.

2.D.1 TRNSYS Simulation Details

The simulated system consisted of a collector, modeled using ASHRAE 93-1977 test data fitted to a straight line, a pump and differential controller with 5 C on and 0.5 C off deadbands and a fully mixed storage tank of 0.310 m^3 volume 1.3 m high insulated to a conductance of 1.7 W/m^2-C. Typical Meteorological Year data was uded to drive the simulation. A 20 hour cycle was run starting the 1 AM with the tank at 25 C.

A number of simulation runs were made in order to test the effects of different system variables on the data reduction procedure. Variables examined in this way included collector area, thermal performance, optical efficiency, pipe losses and time of year.

2.D.2 Effect of Collector Area and Season

The first six simulation runs tested the effect of collector area and season on calculated loop performance. These runs did not include effects of pipe losses or variations in collector optical efficiency. Thermal performance data were used which represented a good quality single cover, selective surface collector ($F_r\ (\tau\alpha)_n = 0.74$; $F_rU_l = 4.44\ W/m^2 - C$). Runs were made with areas of $5m^2$ and $10m^2$ using data from April 1, July 1, and October 1. The results of these six runs are summarized in Table 2.D.1.

Results of Simulated SDHW Tests

Run	Day	Area m^2	$F_r(\tau\alpha)$	F_rU_l W/m^2-C	std.dev.
1	July 1	10	0.739	4.5	0.0101
2	July 1	5	0.740	4.6	0.0091
3	April 1	10	0.741	4.5	0.0128
4	April 1	5	0.742	4.5	0.0082
5	October 1	10	0.735	4.4	0.0176
6	October 1	5	0.739	4.5	0.0175

Table 2.D.1. Results of simulated SDWH system tests using collector with $F_r\ (\tau\alpha)_n = 0.74$ and $F_rU_l = 4.44$ $W/m^2 - C$.

As can be seen, the agreement between test results and actual loop performance is excellent. Since the simple collector model used in these runs is a function only of the collector loop operating point, $\Delta T/I$, any variation of calculated performance from the input parameters must be caused by the calculation procedure itself. Actually, there are several factors tending to make agreement less than perfect. Among these factors are lack of closure of TRNSYS energy balances on a timestep-by-timestep basis, errors in transmission of data and effects due to the representation of tank temperature as average values over timesteps. The first two factors cited above are controllable through use of tighter error tolerances in TRNSYS simulations and parity bits and/or checksums during data transmission. In order to understand the last factor, however, we must understand how TRNSYS represents the tank temperature and its effect on the data reduction algorithm.

Consider two equal and successive timesteps with the associated values of I_t, T_{tnk}, T_{env} and T_{amb}. TRNSYS outputs average values of these quantities at the end of each timestep. Figure 2.D.1 is a plot of tank temperature vs time for these two timesteps. Two

tank temperatures are associated with each timestep. These are represented by $\bar{T}$, the timestep average temperature and T', the timestep endpoint temperature. The change in internal energy of the tank over a timestep is proportional to the difference between the endpoint temperatures of the current and succeeding timesteps. Since TRNSYS only provides the timestep average temperature, the endpoints must be estimated by averaging successive values. This estimate is exact if succeeding timesteps have the same value of $dT/d\tau$. As timestep-to-timestep variations in $dT/d\tau$ become greater, so too does the error in a linear estimate of T'. As can be seen in Figure 2.D.1, the estimated value of T'_2, T''_2, is higher than the actual value of T'_2. As a result, the estimated change in internal energy of the tank will be greater than the actual value. The data reduction algorithm then uses this over-large value to calculate collector loop efficiency, where it occurs in the numerator of Equation 2.B.4. The calculated loop efficiency will be greater than the actual value corresponding to the average operating point for the timestep. This effect will be reversed when the value of $dT/d\tau$ for a timestep is less than that of the preceeding timestep

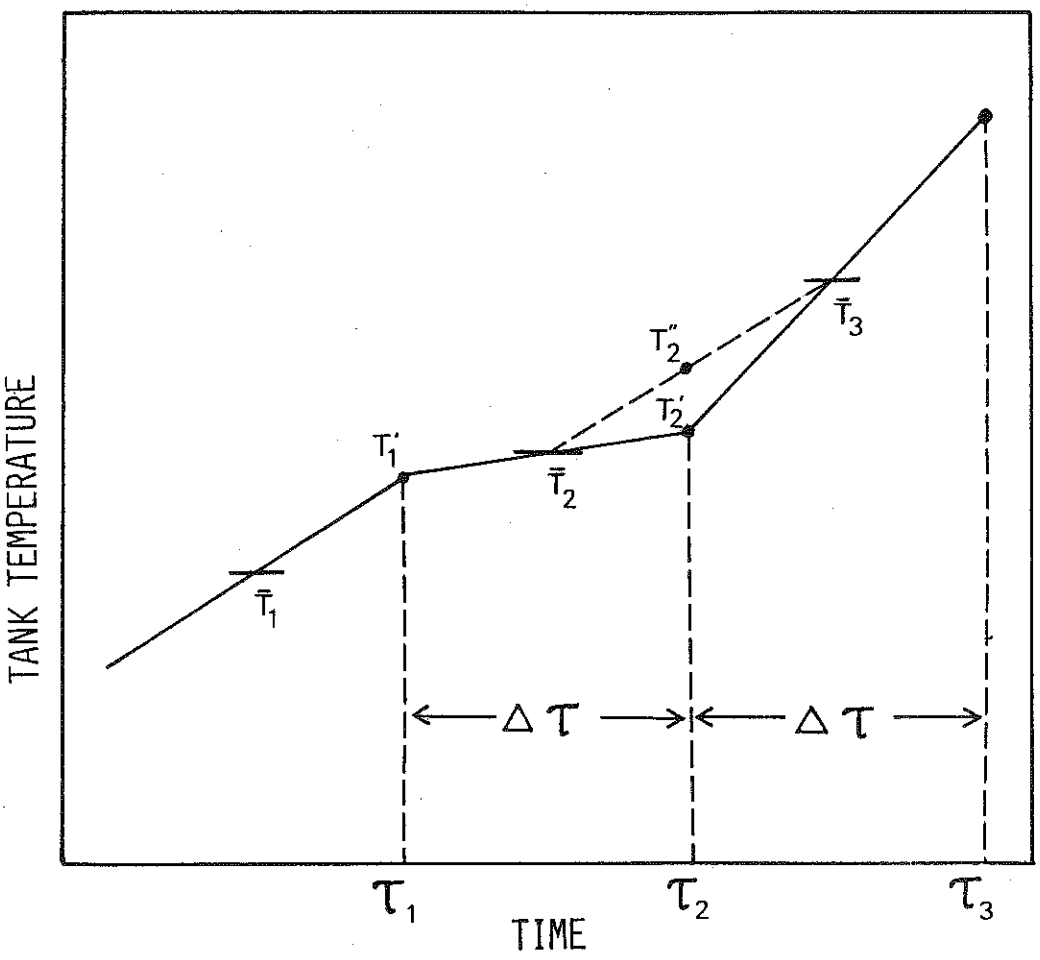

FIGURE 2.D.1. REPRESENTATIVE TANK TEMPERATURE FOR TWO SUCCESSIVE TIMESTEPS, SIMULATED SDHW SYSTEM TEST.

and so result in an underestimation of collector loop efficiency.

The problem outlined above will be aggravated by sudden changes in insolation level which will bring about rapid changes in tank temperature and increase the error in estimating endpoint temperatures. An obvious solution is to decrease the timestep and so decrease the change in slope from one timestep to the next. This solution has its limitations, however, as the change in tank temperature may become too small to resolve over one timestep.

On this basis, days which have rapidly changing insolation levels should yield test results with a greater variance than those with a uniform insolation pattern. This is borne out by the test results in Table 2.D.1, where the runs using October 1 data exhibit greater standard deviation than the other runs. A visual inspection of the tilted surface insolation data for each day (Figure 2.D.2) shows wider variability in the October 1 data than in that for April 1 and July 1.

2.D.3 Effect of Varying Optical Efficiency

The effect of varying optical efficiency was examined by varying the ($\tau\alpha$) product as a function of

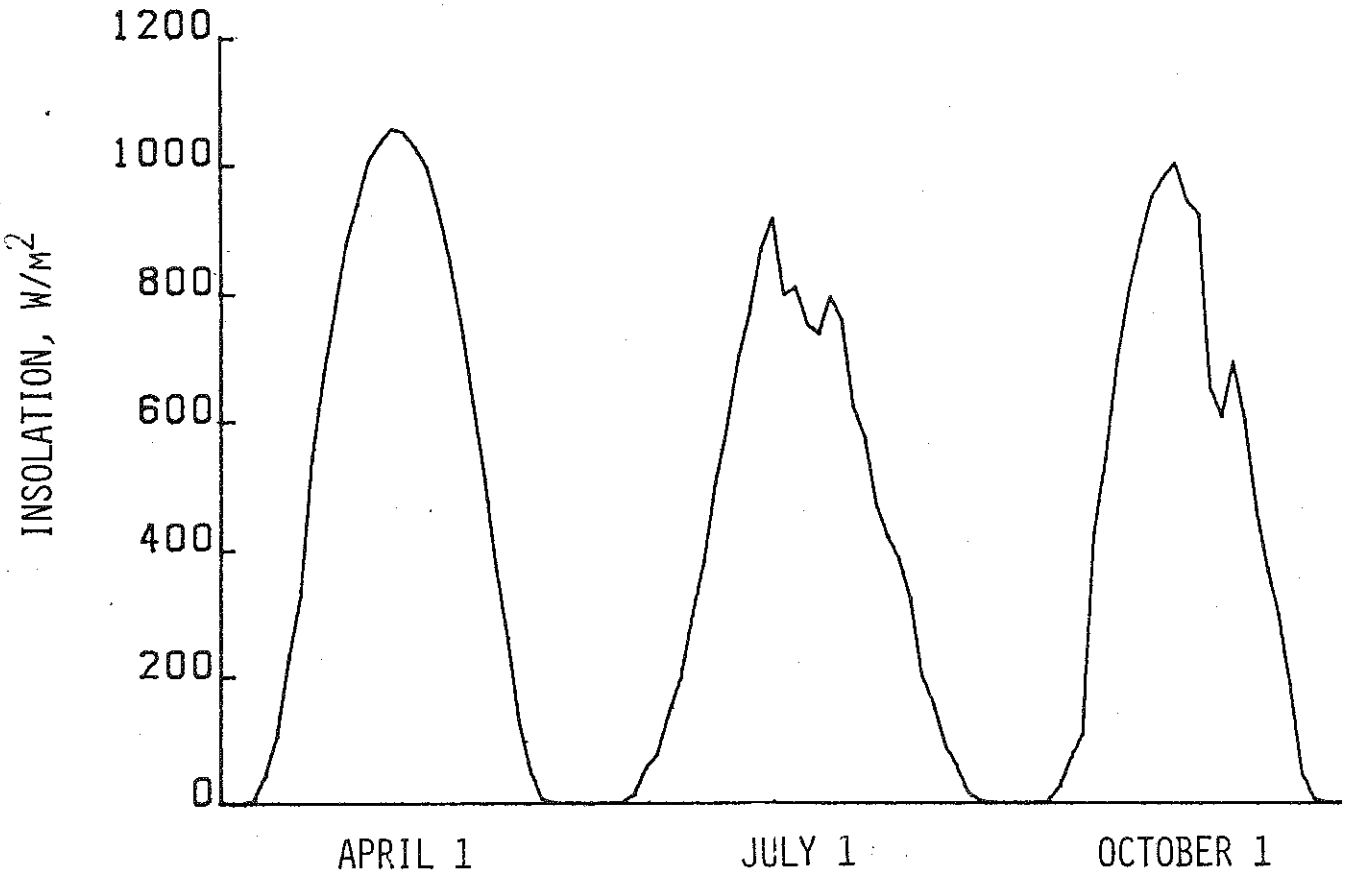

FIGURE 2.D.2. TILTED SURFACE INSOLATION PROFILES USED IN SIMULATIONS OF SDHW SYSTEM TESTS. MADISON, WISCONSIN, SLOPE = 45^{0}

beam radiation incident angle using the function:

$$\frac{(\tau\alpha)}{(\tau\alpha)_n} = 1.0 + b_0 \, (1/\cos\theta - 1) \qquad (2.D.1)$$

Where:

$(\tau\alpha)$ is the collector transmittance-absorptance product at an incident angle of θ,

$(\tau\alpha)_n$ is the collector transmittance-abosorptance product at normal incidence,

b_0 is the collector incident angle modifier,

θ is the incident angle of beam radiation ($0 < \theta < 60$).

This equation is recommended by ASHRAE for regressing optical efficiency vs incident angle data generated by the 93-1977 test procedure [5].

A value of -0.1 was chosen for b_0 as representative of a single cover collector. Three simulations similar to runs 2, 4, and 6 in Table 2.D.1 were performed using this value. The data from these simulations were reduced in the same manner as the previous runs and are reported in Table 2.D.2. The error of the performance estimates has increased considerably, indicating the necessity of including a correction for optical efficiency in the data reduction

procedure.

This correction is accomplished by defining a 'virtual' collector which has constant optical efficiency equal to that of the actual collector at normal incidence. Interposed between the aperture of this collector and the sun is a layer of material which has a varying optical efficiency represented by Equation 2.D.1. The radiation incident on the virtual collector is then:

$$I_r = (\tau\alpha)/(\tau\alpha)_n \, I_t \qquad (2.D.2)$$

Where:

I_r is the radiation received by the virtual collector,

I_t and $(\tau\alpha)/(\tau\alpha)_n$ have been previously defined.

The value of I_r is used in equation 2.B.4 in place of I_t. Results of this modified procedure are shown in Table 2.D.3. These results show much better agreement than the previous set (Table 2.D.2) although not quite as good as those from the first set of runs (Table 2.D.1). This is due to the fact that the data reduction algorithm treats all incident radiation

equally (as beam) whereas TRNSYS calculates different optical efficiencies for beam and diffusely incident radiation components. The neglect of this point by the data reduction procedure is justified by the fact that resolution of beam and diffuse radiation components on site would be costly and overly complex for the simple data acquisition system contemplated.

Results of Simulated SDHW Tests
Varying Optical Efficiency, Uncorrected

Run	Day	Area, m^2	$F_r(\tau\alpha)$	F_rU_l, W/m^2-C	Std. Dev.
7	July 1	5	0.708	4.95	0.0243
8	April 1	5	0.748	5.11	0.0278
9	October 1	5	0.731	4.83	0.0236

Table 2.D.2. Uncorrected results of simulated SDHW system tests using collector with $F_r(\tau\alpha)_n = 0.74$, $F_rU_l = 4.44$ W/m^2 - C and $b_0 = -0.1$.

Results of Simulated SDHW Tests
Varying Optical Efficiency, Corrected

Run	Day	Area, m^2	$F_r(\tau\alpha)$	F_rU_1, W/m^2-C	Std. Dev.
7	July 1	5	0.738	4.50	0.0101
8	April 1	5	0.737	4.51	0.0140
9	October 1	5	0.734	4.54	0.0187

Table 2.D.3. Corrected results of simulated SDHW system tests using collector with $F_r(\tau\alpha)_n = 0.74$, $F_rU_1 = 4.44$ W/m^2 - C and $b_0 = -0.1$.

2.D.4. Effect of Pipe Losses

The last effect to be examined through simulation was that of pipe losses and capacitance. The results reported in Table 2.D.4 include the effects of 30.4 m of 0.022 m diameter pipe insulated with 0.027 m thick nominal mineral wool, k = 0.0364 W/m-C. These runs also include the effects of varying optical efficiency. The piping was divided evenly between the inlet and outlet of the collector. Duffie and Beckman

[1] outline a procedure to modify collector thermal performance to account for losses from pipes exposed to ambient conditions. The expression used for modifying the ($\tau\alpha$) product is:

$$\frac{(\tau\alpha)'}{(\tau\alpha)} = \frac{1}{1 + \dfrac{(UA)_o}{(\dot{m}\ Cp)_c}} \qquad (2.D.3)$$

neglects pipe capacitance

Where:

$(UA)_o$ is the modified transmittance-absorptance product (normal incidence),

$(u\ \Delta\ )_o$ is the conductance-area produce of the outlet piping,

$(\dot{m}\ Cp)_c$ is the thermal capacitance rate of the collector loop.

The overall collector loss coefficient is modified by the factor:

$$\frac{U_l'}{U_l} = \frac{1 - \dfrac{(UA)_i}{(\dot{m}\ Cp)_c} + \dfrac{(UA)_i + (UA)_o}{A_c\ F_r\ U_l}}{1 + \dfrac{(UA)_i}{(\dot{m}\ Cp)_c}} \qquad (2.D.4)$$

Where:

U_l' is the modified collector loss coefficient,

2.E.1 Physical Variables

The system variables required by the algorithms of section 2.B are: bulk average storage tank temperature, tank enviroment temperature, ambient temperature, collector loop inlet and outlet temperatures, collector surface insolation, pump status and time of day. For the small storage tanks (under 0.5 m^3 in volume) encountered in SDHW systems, three separate measurements of tank temperature, averaged together, are representative of the bulk average value. This brings the number of temperature measurements to seven.

Collector surface insolation may be measured by a silicon-cell based device which generates a frequency encoded output. Pump status may be measured by the same method, with the output signal developed from the 60 Hz waveform of its power source. Time of day may be derived from a crystal-controlled clock.

2.E.2 Measurement Error Sensitivity Analysis

The sensitivity of the data reduction algorithms to measurement error was estimated by adding two error terms to the temperature and insolation data output by the TRNSYS simulation used in section 2.D. The error terms were made up of a random component and a fixed component. The temperature values used in the data

reduction procedure were:

$$T_m = T + T\ (p)\ (0.5 - rnd) + eT \qquad (2.E.1)$$

T_m is the modified temperature value, T is the actual (reported) temperature, p is the maximum error magnitue, rnd is a random number between 0 and 1 and eT is a fixed error in units of temperature.

A similar procedure simulates errors in insolation measurment, with insolation estimated as:

$$I_m = I_t + I_t\ (q)\ (0.5 - rnd) + eI \qquad (2.E.2)$$

I_m is the modified insolation value, I_t is the actual insolation value, q is a maximum percentage error in insolation measurement and eI is the fixed insolation error term.

The effects of the different error terms were explored using an experiment based on a two level factorial design in four variables. The variables used were 1) random temperature error, 2) random insolation error, 3) fixed temperature error and 4) fixed insolation error. The following table lists these variables and the high and low values chosen for them.

Variable	Symbol	Low Value (-)	High Value (+)
random temperature error	x1	+/- 0.0 C	+/- 0.25 C
random insolation error	x2	+/- 0.0 %	+/- 3.0 %
fixed temperature error	x3	0.0 C	- 2.0 C
fixed insolation error	x4	0.0 W/m^2	+ 55.6 W/m^2

Table 2.E.1. Values of error terms used in sensitivity analysis.

The experiment requires 6 test runs. These runs used the data from TRNSYS simulation run 15, Table 2.D.1, with added error terms. The response was the standard deviation of the fitted straight line. Data from the 16 runs are presented, with an analysis of effects, in Table 3.E.2.

	variables				response	analysis	
Run	x1	x2	x3	x4	std. dev.	effect	avg. std. dev.
1	-	-	-	-	0.015	avg	0.066
2	+	-	-	-	0.108	x1	0.095
3	-	+	-	-	0.023	x2	-0.003
4	+	+	-	-	0.113	x3	-0.002
5	-	-	+	-	0.015	x4	-0.003
6	+	-	+	-	0.123	x1x2	-0.006
7	-	+	+	-	0.019	x1x3	-0.000
8	+	+	+	-	0.017	x1x4	-0.001
9	-	-	-	+	0.019	x2x3	-0.002
10	+	-	-	+	0.128	x2x4	-0.001
11	-	+	-	+	0.022	x3x4	-0.002
12	+	+	-	+	0.109	x1x2x3	0.000
13	-	-	+	+	0.019	x1x2x4	-0.001
14	+	-	+	+	0.111	x2x3x4	0.006
15	-	+	+	+	0.022	x1x3x4	-0.005
16	+	+	+	+	0.108	x1x2x3x4	0.004

Table 2.E.2 Experimental design, results and anlysis of error sensitivity experiment.

The 'noise' level in this experiment can be estimated from the root mean square of the 3- and 4-factor interactions, giving a value of 0.004. The only effect significantly larger than this value is that of random temperature error, x1 in Table 2.E.2, which leads to the conclusion that, for the range of variable examined, this variable has the greatest influence on the goodness of fit experimental data to a straight line.

Temperature offset error, represented by x3 in Table 2.E.2, does not have a large effect on the goodness of fit. This conclusion is important in that

it is much easier to measure tank temperatures using surface-mounted sensors. However, a surface-mounted sensor reading will include an error relative to the actual fluid temperature. An examination of Equation 2.B.4 shows that this error, if constant over time, will cancel out of the internal energy term.

Tank loss estimates will be affected by fluid temperature measurement errors. However, tank losses are small compared to internal energy changes. As a result, errors in estimating tank losses do not have a marked effect on the goodness of fit of the regression. Random error, on the other hand has a marked effect on the goodness of fit. The +/- 0.25 C high level used in the experiment above more than doubled the regression's standard deviation. Low-cost commercially available temperature measurement systems have uncertainties on the order of +/- 1.0 C or worse. If this type of system was used to acquire data for SDHW tests, the results would be swamped by noise.

The Cental Limit Theorem indicates that the standard deviation of a set of values may be reduced by averaging within the set [30]. Using this property, it is possible to reduce the uncertainty in temperature values by averaging a large number of individual

samples. This concept was used in designing the temperature sensor sub-system discussed in the following chapter.

It appears that the data reduction algorithm can tolerate random error in insolation measurement of up to +/- 3% of the value. In addition, the absolute error simulate above is about 4% of the maximum possible intensity of 1353 W/m^2. These error values are close to those for commercially available silicon-cell based radiometers of the type used in the DAS detailed in the next chapter.

Chapter 3

SDHW Data Acquisition System

3.A Introduction

The data acquisition system consists of a microcomputer and several peripheral devices. As indicated in the previous chapter, this system must perform the following tasks:

1) Acquire temperature data from seven locations;
2) Sense and integrate solar radiation intensity;
3) Sense pump on/off status;
4) Keep track of real time-of-day;
5) Save data to disk file at specified intervals.

An additional function, the reduction of data in real time, is desirable but adds greatly to the complexity of the system. As implemented, the system does little real time processing of data but provides for the reduction of data after testing is concluded.

The DAS is built around an Apple][Plus microcomputer and includes hardware for sensing temperature, solar radiation, pump status and real time. System software integrates and sychronizes the

hardware functions and provides data display and recording facilities.

The following sections will first discuss the system hardware functions followed by a description of the software.

skipped to pg 107

3.B System Hardware Components

3.B.1 Apple][Plus Microcomputer

The Apple][Plus Microcomputer used in the DAS is built around the 8-bit 6502 processor and includes 48,000 bytes of read/write memory, 12,000 bytes of read only memory, a keyboard, video display and mini-floppy disk storage with a capacity of 130,000 bytes. The Apple includes seven useable peripheral slots on its main circuit board, each of which has access to the system's address, data and status lines.

Software supplied with the Apple system includes a BASIC interpreter supporting floating point, integer and character string data types. This software is resident in read only memory along with routines to carry out primitive input/output functions such as keyboard and video display.

The Apple's mini-floppy disk is supported by software resident in read/write memory. This code, known as the Disk Operating System (DOS), is read in

from the disk when the Apple is powered-up or when an initialization command is received. The DOS supplied with the Apple is very primitive and is not well interfaced to the resident BASIC interpreter.

The Apple II was chosen on the basis of price, availability and quality of documentation. The last point is very important, since integration of a real-time DAS with an off-the-shelf microcomputer requires a detailed knowledge of a system's hardware and software. The documentation supplied by Apple Computer, Inc. includes up-to-date schematics and detailed discussions of the theory of operation of most main circuit board components. The Apple's DOS is not as well supported by the manufacturer. This is made up for by publications available from outside vendors [31].

The hardware and software described in the following sections could be adapted to any microcomputer providing that the proper interface modules were available. Since the DAS was developed during the latter part of 1981, quite a few high quality analog interface units have appeared on the market. These units are adaptable to a wide range of microcomputers and make the task of implementing a DAS

much simpler.

3.B.2. Temperature Sensor Sub-System

At the time that the DAS was being specified (Fall, 1981), only two temperature sensing peripherals were available for the Apple. One of these involved an external unit with its own power supply and enclosure. This unit used thermocouple transducers and was relatively expensive (more than $1500). Although it could supply temperature readings at a high data rate with acceptable accuracy, this system was rejected on the basis of its bulk and cost.

The second type of temperature sensor available at the time was a two-channel unit which was self-contained and inexpensive. However, the accuracy of the unit was questionable. In addition, four units of this type would use up too many of the Apple's peripheral connector slots and overload the internal power supply.

The only course left was to build a temperature sensing subsystem out of off-the-shelf data converters and custom-built signal conditioning circuits.

This sub-system uses a 16 channel analog-to-ditital (A/D) and digital-to-analog (D/A) data converter manufactured by Mountain Computer, Inc. The

A/D-D/A unit has eight bit resolution and converts analog data to digital form in only 10 microseconds, allowing the high sampling rate required to implement signal averaging schemes.

Several issues were addressed in developing the temperature sensing sub-system, including transducer type, resolution, calibration and stability.

Transducer types fall into three categories: thermocuple, resistance and semiconductor junction.

Thermocuples are widely available in standard types and are relatively easy to handle and apply. However, their sensitivity is very low, on the order of microvolts per degree C, requiring high-gain amplifiers, extensive shielding and data converters with high resolution (e.g., 12 to 16 bits). In addition, some type of reference device is needed to achieve good accuracy. These factors prohibit their use in the low-cost system under consideration.

Resistance type temperature transducers are really of two distinct types: resistance temperature detector (RTD) units and thermistors. RTD devices are constructed of platinum-rhodium or other alloys and are bulky and expensive ($50 and up per sensor). These factors are sufficient to remove RTDs from

consideration in this application.

Thermistors are widely used as temperature sensors and have many good features, including small size. However, thermistor response is non-linear and self-heating effects can cause significant errors. Another problem is the ageing of units is service with accompanying change in characteristics. Finally, quality, pre-aged, thermistors with well-documented parameters are fairly expensive, going for $25 and up in 1981.

Semiconductor junction devices have good sensitivity, on the order of 1 mV/C and are highly linear in the 0-100 C temperature range encountered in SDHW systems. Although several types of devices are available commercially, good results can be obtained from an ordinary NPN transistor connected as a diode [32]. Excitation currents for this type of device are about 100 micro-amps and can be provided by the 5 volt supply internal to the Apple. For these reasons, ordinary plastic-encapsulated NPN transistors were chosen as temperature transducers.

The 2 mV/C sensitivity of p-n junction devices implies a 0.2 volt swing in output from 0 C to 100 C. Since the A/D-D/A card in the Apple has a full-scale

range of -5 to +5 volts, some type of pre-amplification is required. In addition, the eight-bit data converter has a resolution of 1 in 2^8 (1 in 256). this translates to a resolution of +/-0.25 C, at best. The sensitivity analysis of the previous chapter implied that temperature resolution must be on the order of +/-0.25 C to give good results.

The resolution and range problems were solved by using the circuit of Figure 3.B.1. This circuit uses a pair of monolitic operational amplifiers operating in the differential mode to provide a reference, amplification and range offset functions. The first amplifier, A1, has a voltage gain of 20 and is used to amplify the transducer output relative to a fixed low-noise reference voltage. The output of A1 is sent to the inverting input of amplifier A2, which is a second gain-of-20 unit identical to A1. The non-inverting input of A2 is connected to the output of one of the D/A converter channels. The differential configurtion of A2 allows the D/A output to be used as an offset to bring the circuit's output within the +5 to -5 volt range of the A/D input.

In operation, software in the Apple examines the A/D channel output. If the value is under - or over-

range, the corresponding D/A convertor's output is raised or lowered and the A/D channel output is again checked. This process continues until the A/D output is within the required range. At this point, the A/D output and the last D/A value are added to values previously stored in the Apple's memory and scanning proceeds to the next channel. Separate two-byte locations hold the running total of the A/D and D/A readings from each channel. After a preset number of scans (ten or more) of all channels, the scanner routine returns to its caller. The interaction of this and other software in the system allows ten readings per second from each temperature sensing channel. In a five minute interval 3000 temperature values can be accumulated and averaged from each of the eight channels, greatly reducing the random error in any one five minute average temperature value.

The transfer function of the system is:

$$T = \frac{(x-x_o) - b_2(r - r)}{b_1} + T_o \qquad (3.B.1)$$

T is the temperature sensed, x is the A/D channel reading, X_o is the reference A/D channel reading, r is the D/A channel setting, r_o is the reference D/A

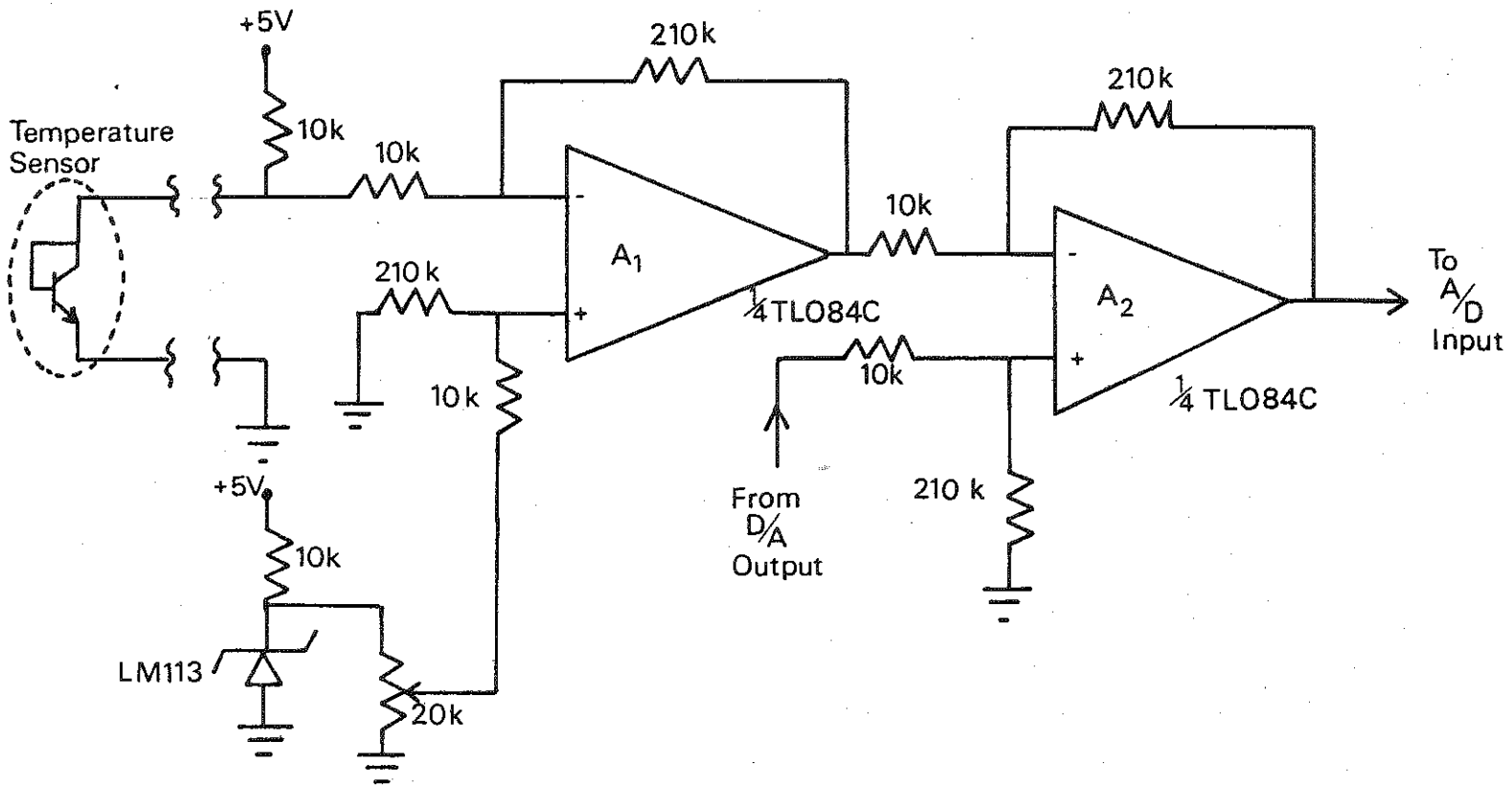

FIGURE 3.B.1. SCHEMATIC DIAGRAM OF TEMPERATURE SENSOR INTERFACE.

channel setting, T_o is the reference calibration temperature, b_1 and b_2 are calibration constants.

The constants b_1 and b_2 can be found by re-arranging 3.B.1 into the form:

$$x - x_o = b_1(T-T_o) + b_2(r-r_o) \qquad (3.B.2)$$

if this is differentiated with respect to x, the result is:

$$dx = b_1\, dT + b_2\, dr \qquad (3.B.3)$$

the constants b_1 and b_2 can be determined by finding:

$$b_1 = dx/dT \ (r = \text{constant}) \qquad (3.B.4)$$

$$b_2 = dx/dr \ (T = \text{constant}) \qquad (3.B.5)$$

The sensors can be calibrated in two steps. The first step finds b_2 by holding T constant, varying r and finding the average of the ratio:

$$b_2 = (x - x_o)/(r - r_o) \qquad (3.B.6)$$

for all values of r which allow x to be less than full scale and greater than zero. (This process is really finding the gain of amplifier A2.)

Constant b_1 may be found by shifting the temperature sensor to an environment of a widely different, known, temperature. The constant b_1 may be found by using the expression:

$$b_1 = \frac{(x - x_o) - b_2(r - r_o)}{(T_1 - T_o)} \qquad (3.B.7)$$

$T_1 - T_o$ is the difference between the sensor temperature during the first step (finding b_2) and the current step.

This procedure yields five calibration values for each temperature channel: x_o, r_o, T_o, b_1 and b_2. Calibration values are stored on disk along with calibration date and a comment tag.

Generating the calibration values and writing the calibration file is simplified by a menu-driven program which also allows screen display of temperature sensor output.

The temperature sensing sub-system is synchronized by the DAS system executive software, described in Section 3.C.1.

3.B.3 Temperature Sensor Installation

Since the data acquisition system is intended for use on existing systems without special provisions for temperature monitoring, surface mounted tank and pipe temperature sensors were used. The use of surface mounted sensors also does away with any need to open the SDHW system's piping and simplifies the installation of the DAS on the system under test.

Surface-mounted sensors on the tank are inserted through 0.0095 m (3/8 inch) holes in the steel jacket of the tank, through the insulation layer, a nominal 2 inches of chopped glass fiber, and make contact with a prepared section of the tank shell. Surface preparation consists of scraping off paint and scale and applying a layer of generic silicone heat sink compound.

The sensor itself is a plastic-encapsulated NPN general purpose transistor. The case is the TO-92 type with gold-plated nickel leads extending 0.015 m (5/8 inch) to one side. All three leads, at a short distance from their ends, are bent around the 20-gage stranded connecting wires. The connection is soldered and encased in two layers of heat-shrink tubing so that the upper half of the plastic encapsulation is

exposed. The sensor is inserted so that the tip of the package contacts the tank shell. In later tests, the hole through the tank jacket was 'cased' with a short piece of plastic tubing to ensure that the sensor contacted the tank head-on and was firmly held in place by tape on the lead wire. In the MG&E tests, this was not done, although the sensors were held fairly straight in place by tape.

The point the sensor wire penetrates the tank jacket is covered with several layers of self-stick foil-backed foam pipe insulation 0.004 m thick.

A simplified thermal circuit of the sensor installation is shown in Figure 3.B.2. The circuit has been simplified by neglecting capacitance effects and considering one-dimensional heat transfer only. The sensed temperature, T_s, is determined by the relative magnitudes of the sensor-to water heat transfer resistance, R_{ws}, and the sensor-to ambient heat transfer resistance, R_{sa}. the relationship is:

$$T_w - T_s = \frac{R_{ws}}{R_{ws} + R_{sa}} (T_w - T)_a \qquad (3.B.8)$$

As R_{ws} decreases, the error in water temperature decreases, going to zero at $R_{ws} = 0$. Conversely, as

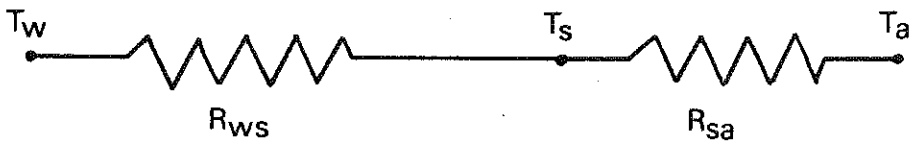

FIGURE 3.B.2. THERMAL CIRCUIT OF SURFACE MOUNTED TEMPERATURE SENSOR.

R_{ws} increases, the error increases to an upper bound of $(T_w - T_a)$.

Measurements taken on a gas-fired water heater showed a reading of 61 C at a point on the tank 1/4 of the way down from the top. A simultaneous reading of tap water drawn from the tank showed a temperature of 64 C. The tank ambient was at a temperature of 27 C. Using Equation 3.B.8, the ration of R_{sa} to R_{ws} can be estimated to be around 11 to 1.

The rough experiment described above implies that the tank temperature error will be about 10% of the tank to ambient temperature difference.

Pipe surface temperatures were sensed in a similar fashion, the sensor taped tightly to a section of copper pipe prepared with a coating of heat sink compound. The assembly was covered with a layer of nominal 2 inch foam rubber insulation.

Measurements taken on copper tubing containing flowing water showed an error of less than 1 C between the mixed water temperature and the pipe surface temperature.

The lower error in sensing flowing fluid temperature is due to the lower heat transfer resistance between the fluid and the sensor, a result

of better sensor-to-pipe contact and a higher film coefficient of heat transfer between the flowing water and the inner pipe wall.

3.B.4. Frequency Encoded Transducer Interface

The solar radiation and pump status transducers generate frequency encoded outputs which are interfaced to a programmable timer card model 7440 manufactured by California Computer Systems. This card contains a Motorola MC6840 programmable timer chip (PTC) and circuitry to interface it to the Apple expansion connectors.

The MC6840 [33] contains three independent 16-bit registers which may be programmed to operate in either counter or timer mode (among others). The DAS uses two of these registers in counter mode to interface with the radiometer output and pump satus signal. The third register is used in timer mode as a 'tick' generator to synchronize temperature sensor scanning and other DAS system functions.

In operation, the PTC registers are initialized to a value between 0 and 65535. In timer mode, this initial value is decremented each time a system clock pulse is received. In counter mode, the register is decremented on receipt of an external pulse. As used

in the DAS, the PTM channels generate a processor interrupt when they reach a zero count. The interrupts are serviced by the DAS Executive, which identifies the source and takes appropriate action. Operation of the DAS Executive is detailed further in section 3.C.1.

3.B.4.a Solar Radiation Transducer

The solar radiation transducer chosen for the system was manufactured by Hollis Observatory, Nashua, New Hampshire. The sensing element is a single-crystal silicon photovoltaic cell and is encapsulated with a signal conditioning network which generates a square wave output proportional to incident solar intensity. The calibration constant is 10 HZ-m^2W. The device is accurate to within +/- 4.0% of the actual value over the 0-1400 W/m^2 range, according to the manufacturer. This value is for solar radiation incident at less than 70 degrees to the normal axis of the device and having a spectral content corresponding to atmospheric conditions of air mass one.

A frequency-encoded silicon-cell based transducer was chosen on the basis of the simplicity of signal transmission and interfacing as well as cost.

The radiometer is clamped to the collector frame during system testing. Alignment screws on the base

are used to set the sensing element aperture parallel to the plane of the collector cover.

Radiometer output and power supply (nominal 12 VDC) connections are carried in a 3-wire cable to the DAS unit. A simple signal conditioning circuit, shown in Figure 3.B.3, 'cleans up' the output before it is delivered to the counter timer chip.

The PTC register associated with the radiometer is preloaded with a value of 5000. When this register decrements to zero and generates an interrupt, the radiometer has received a total of 500 J/m^2 of energy. This represents the integral of th transducer's frequency output of 10 $Hz\text{-}m^2/W$ over the elapsed time. The time period between interrupts varies from many hours (dark response) to once every 2.6 seconds at a solar intensity of 1300 W/m^2. The DAS Executive software uses the number of radiometer interrupts and the residual PTC register contents to calculate data scan interval average solar intensity.

3.B.4.b. Pump Status Sensor

The on-off status of the circulating pump is sensed by the circuit shown in Figure 3.B.4. This circuit uses an optoisolator connected across the pump power leads to generate a 60 Hz logic level signal when

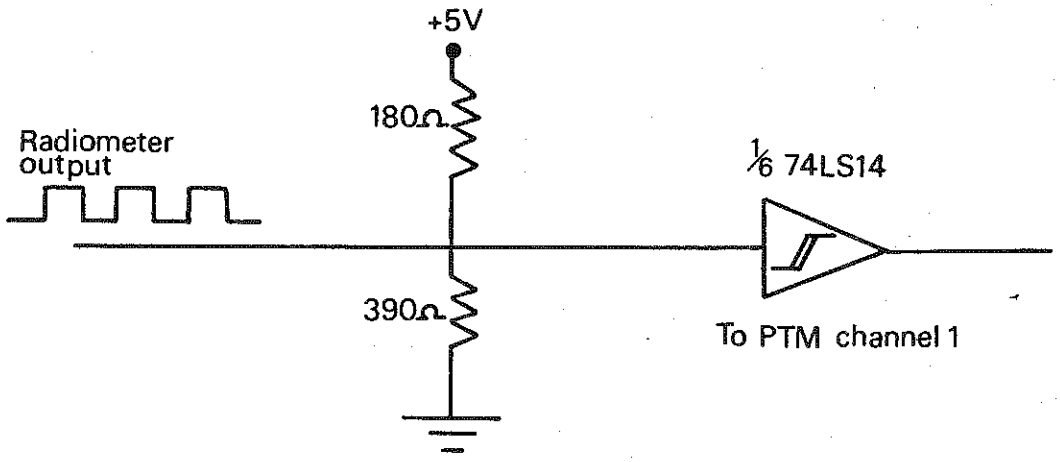

FIGURE 3.B.3. SCHEMATIC DIAGRAM OF RADIOMETER OUTPUT SIGNAL CONDITIONING CIRCUIT.

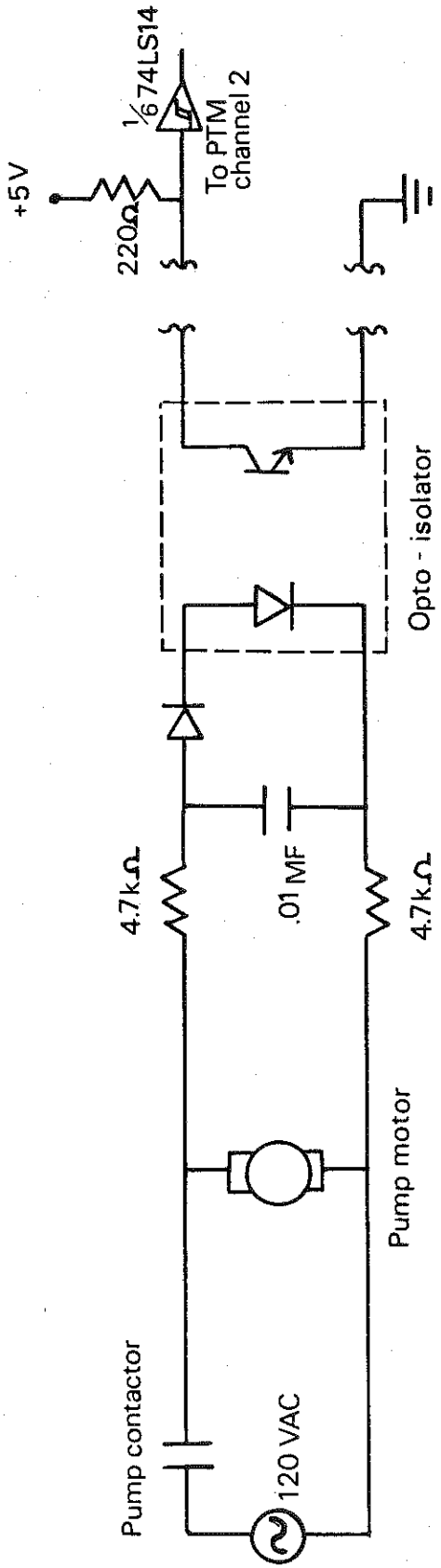

FIGURE 3.B.4. SCHEMATIC DIAGRAM OF PUMP STATUS SENSOR CIRCUIT.

the pump is on. The optoisolator consists of a light emitting diode (LED) which activates a phototransistor. The LED and transistor are isolated from each other by a layer of clear plastic with a high breakdown voltage. The assembly is potted in an opaque plastic enclosure. The LED is powered by the 60 Hz power supplied to the pump. During each positive cycle of the 60 Hz input the LED illuminates the phototransistor, causing it to conduct current. The resulting signal is connected to a PTC register input.

When the pump is on, the pump status PTC channel generates an interrupt for every 600 pulses received. This interrupt represents 10 seconds of pump operation. Pump operating time, in 10 seconds units, is recorded by the DAS Executive for processing by other system software modules, as will be discussed later.

3.B.5 Real Time Clock Hardware

The system's real time clock is on the CPS Interface card manufactured by Mountain Computer, Inc. The unit includes a battery and other circuits which keep the clock running even when the system is powered down. Time resolution is one second.

The CPS card's interface to the system is handled

by on board software proprietary to Mountain Computer. This software relies on timing loops which cannot tolerate interrupts during execution, so that all data acquisition operations must be halted while the clock is being read. In order to prevent data loss, the system software is designed to read the real time clock only when updating disk files or screen displays.

3.C. System Software

3.C.1. Introduction

The DAS real-time software is built up from two modules. The first is the Executive module, implemented in machine code to service interrupts from the radiometer and pump status inputs and scan the temperature sensors. The remainder of the DAS real-time software is implemented in Applesoft BASIC and carries out the tasks of unit conversion, screen display and file maintainence.

Data reduction software is made up of several modules. The first is a data display program which allows graphic or numeric display of data which has been recorded on disk. The next module does analysis of tank losses and collector loop flowrate. The last

module analyzes collector loop performance and heat exchanger effectiveness (for systems with internal heat exchangers).

A utility program to calibrate the temperature sensors is also included.

3.C.2. Executive Module

The Executive module is located in the Apple's memory between the beginning of the Apple DOS and the end of the space reserved for BASIC programs. The DOS was modified to 'hide' this area from the rest of the system to prevent the destruction of its contents during disk I/O operations. When the DAS is initialized, the Executive module is read from disk and placed in this protected area.

A simplified flowchart of the Executive module is contained in Figure 3.C.1. A listing of the assembly language source code of this module is contained in the Appendix. Operation of the Executive code is controlled by the Programmable Timer Module (PTM) on the card in expansion slot 2 of the Apple. The PTM can generate an interrupt in the event that any of its three 16-bit registers reaches a zero count. When the Apple's CPU receives an interrupt, it completes the current instruction cycle and jumps to the interrupt

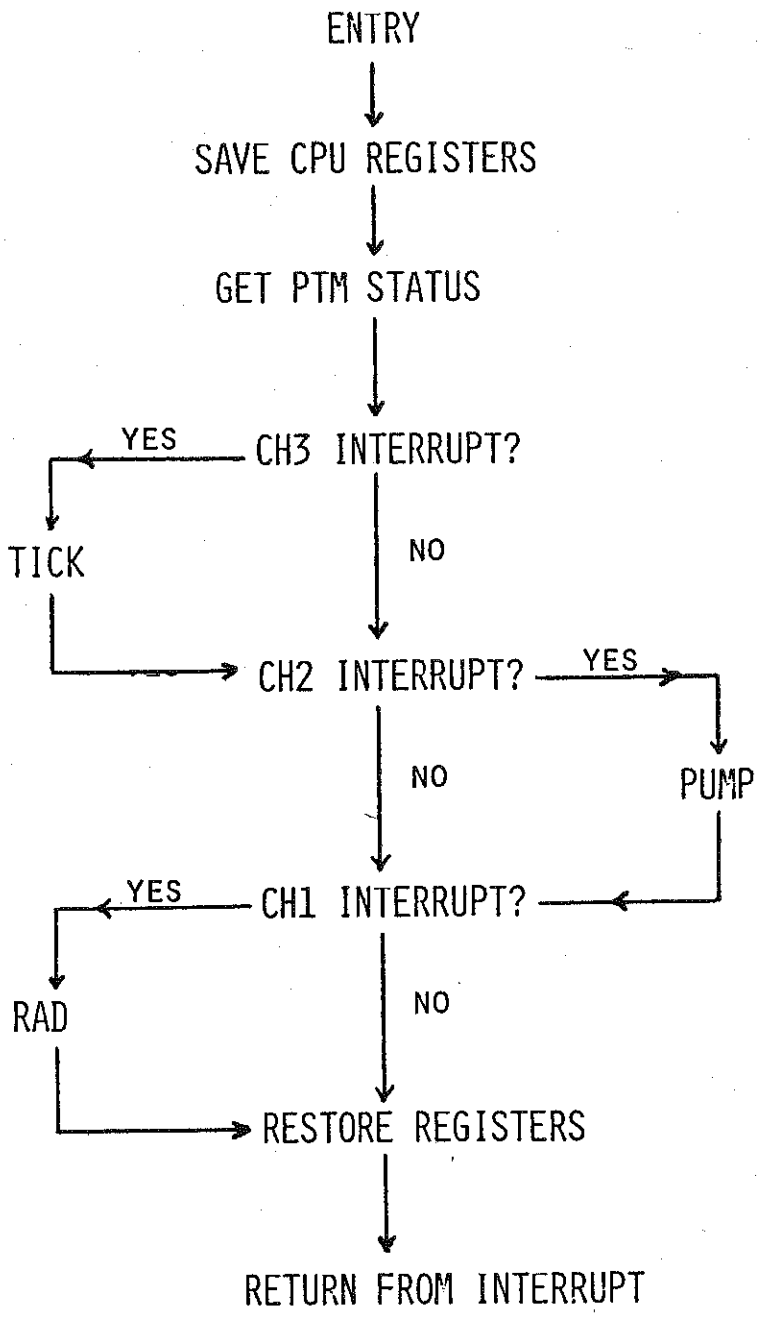

FIGURE 3.C.1. FLOWCHART OF EXECUTIVE MODULE INTERRUPT SERVICE ROUTINE.

service code contained in the Executive module.

Channel 3 of the PTM is connected to the Apple's nominal 1 MHz clock signal through a divide-by-8 prescaler. When the system is initialized, the channel 3 register is set to approximately 12,500. Each eight cycles of the 1 MHz system clock signal decrements this counter by 1. After 100,000 cycles of the system clock, or about 1/10 of a second, the channel 3 register 'times out' and generates an interrupt. This is the 'TICK' interrupt and is used to synchronize all operations of the DAS.

After 10 occurrences of the 'TICK' interrupt, the Executive code calls the temperature sensor scanning code, 'TSCAN'. At the same time, it sets a flag (a single bit in memory) to indicate to the BASIC screen and file interface program that valid temperature data is available.

After a preset number of calls to the TSCAN routine (300 for the tests detailed in Chapter 4), a second flag is set which indicates that a disk file record should be written. The PTM interrupts are disabled at this time to prevent conflicts with the real time clock.

Channels 1 and 2 of the PTM operate independently

of channel 3. Channel 2 is connected to the pump status sensor line. The channel 2 register is preset to a value of 600 so that the 60 Hz pump status signal will generate an interrupt for every 10 seconds of pump operation. This interrupt is serviced by subroutine 'PUMP' which increments a memory location which contains the total number of 10-second intervals the pump has been on.

The radiometer input is connected to channel 1 of the PTM. The input is a square wave with a frequency proportional to radiation intensity. The calibration constant is 10 Hz-m^2/W. The channel 1 register is preset to 5000 so that an interrupt occurs on channel 1 after 5000 pulses from the radiometer or after a total of 0.5 kJ/m^2 of radiation has been received. The subroutine 'RAD' in the Executive module handles radiometer interrupts and operates in a similar fashion to the 'PUMP' routine by incrementing a memory location which is in turn read by the BASIC fle and screen interface program.

3.C.3 BASIC File and Screen Interface

The BASIC file and screen interface program operates in two stages. The first stage, initial data entry, is interactive and allows the user to enter the

measurable SDHW system parameters of collector area, orientation, tank capacity, height and (optionally) insulation 'R' value. The program also prompts the user for entry of temperature sensor assignments, which are a sensor number and a two-letter location identification code for each of the eight sensors. This simplifies the sensor installation task by allowing any sensor to be installed in any location in the system under test.

The initial data entry stage also allows the user to name the disk data file used to record test data. The test data file is a random-access file made up of 128-byte records. Record zero of the file contains system parameter and sensor assignment information. The subsequent records contain system operating data recorded at equal intervals along with a corresponding time stamp. The recording interval is set by user input and ranges from a minimum of 60 seconds to a maximum of 65,535 seconds (18.2 hours). With all the necessary program and data files, the available capacity of the Apple's disk is about 480 sectors of 256 bytes each. Since the data file is made up of 128-byte records, there is room on the disk for 960 records of system operating data. If the minimum data interval

of 60 seconds is used, this allows 16 hours of data collection before the disk fills up. At the other extreme, almost two years of data may be recorded at the maximum interval of 18.2 hours.

After the initial data entry stage is complete, the operator enters a command to start the test run. At this point the program enters its scanning loop. A flowchart of the scanning loop is contained in Figure 3.C.2. On entry to the scanning loop, code is executed which initializes the PTM unit and interrupt system of the Apple's CPU. This enables the tick routine outlined above. The program then enters a loop in which it checks the location TFLAG which is set by the Executive routine after the temperature channels have been read. When TFLAG is set, the program converts the temperature sensor readings to engineering units and sums the resulting values to holding registers. The screen display of seconds to next scan is updated at this time also.

After the temperature sensor values are saved, the program checks location DFLAG which indicates whether a disk record (or scan) is to be written. If DFLAG is not set, the program loops back to checking TFLAG. When DFLAG is set, several events are triggered. The

Chapter 4

System Tests

ms have been tested using the methods and
ribed in the previous chapters. The
was a direct circulation type while the
ndirect type using an in-tank heat
. Both systems required several days of
her the data needed to make a reasonable
eral problems with the DAS and the
dentified during the testing period.
ed to the DAS were corrected as soon as
e system-related problems were solved,
ere only identified and solutions were

ERATURE
ES

NT COUNTER

ES

Gas and Electric System

Description

system tested was located in the Madison
ic (MG&E) central office facility, 120
et, Madison. This system was distributed
Inc. and is made up of parts
y several different companies. The
sified as a direct circulation two-tank

LOOP IN
RAM.

type and provides water to the office staff and a gas meter service shop.

The solar tank used in this system is of nominal 310 l (82 gallon) capacity. The tank shell is 1.37 m (4.5 feet) high with a diameter of 0.43 m (16.9 inches). The shell is covered with a nominal three inch layer of chopped glass fiber and is jacketed in 20 gage steel. The lower head of the tank rests directly on the lower jacket panel which in turn rests on a carpeted concrete floor.

Potable water is pumped from the lower connection of the solar tank directly to the collectors by two Grundfos model UP25-42SF pumps connected in series. The collector supply piping, nominal 3/4" type L, is carried in a pipe chase from the first floor to the roof of the two-story building with a vertical rise of 7 m (23 feet). A further 4 m of pipe is exposed on the roof and connects the two collector modules in series. Only the roof mounted piping is insulated, the insulation consisting of nominal 1" thick foamed rubber in an advanced state of deterioration. The collector return piping follows a path parallel to the supply piping and is insulated in a similar fashion. Water returning from the collectors is delivered to the upper

part of the storage tank through a 'dip' tube extending about 0.5 m (18 inches) into the tank.

Freezing is prevented by allowing the collectors to drain into the storage tank when the circulator pumps are off. This is possible due to the presence of an air space in the upper part of the tank. This air space is maintained by a small air compressor. The system's controller senses the height of the air cushion through two electrodes installed in the upper head of the tank and activates the compressor when the air space is smaller than a minimum value. An interlock in the controller keeps the circulators and air compressor from running simultaneously.

The collector array is made up of two modules manufactured by Solar Development Inc. of Riviera Beache, Florida. The units are connected in series and are mounted on separate racks spaced approximately 2 m apart. The collectors are tilted at 45 degrees with a 10 degree west of south azimuth angle. In addition, the collectors are tilted lengthwise to allow draining. Black painted copper tube-and-sheet construction is used in the absorber unit which is enclosed in a painted steel case backed by 0.025 m of polyisocyanurate insulation and fitted with a

proprietary fiber reinforced plastic cover (Filon). Gross area per module area is 3.53 square meters, aperture area is 3.46 m^2.

The system's auxiliary tank is located in the basement, one floor down from the solar storage tank. The tank is fired with natural gas and has a nominal capacity of 151 l (40 gallons) and is jacketed with 0.025 m of glass fiber insulation. The hot water outlet of the solar storage tank is connected with the auxiliary tank by 3.5 m of pipe covered with 0.025 m of foam rubber insulation.

Hot water is delivered to the building's piping through a temperature-controlled mixing valve and is made up by city mains water supplied to the solar storage tank.

4.A.2. Test Procedure

The MG&E system was tested during two separate periods. The first testing period covered parts of the month of September 1982. The second covered a week in October 1982. Several problems with the data acquisition system, the SDHW system under test and a lack of good weather meant that only three days of usable collector operating data were gathered during the month of September. After these problems had been

identified and corrected, another set of tests were conducted the next month.

The first problems encountered were in the system under test. The first of these was the lack of a bypass valve between the cold water supply and the auxiliary water heater inlet. To preserve 'no-load' conditions in the solar tank, testing could only be done on the weekend, when the building was unoccupied. This problem was corrected late in September.

Data were gathered from Friday night, September 3, through Monday morning, September 6. The 4th was quite sunny, as the radiation plot in Figure 4.A.1 shows.

There are several points to note in Figure 4.A.1. First, the collector loop inlet temperature trace is above the average tank temperature line. If there is any thermal stratification in the tank, the collector inlet temperature should be less than the average tank temperature. This disagreement is due to the use of surface-mounted temperature sensors, discussed in section 3.B.3.

In Figure 4.A.1, the plotted tank average temperature is approximately 3-4 C below the collector inlet temperature measured on the pump outlet line 0.03

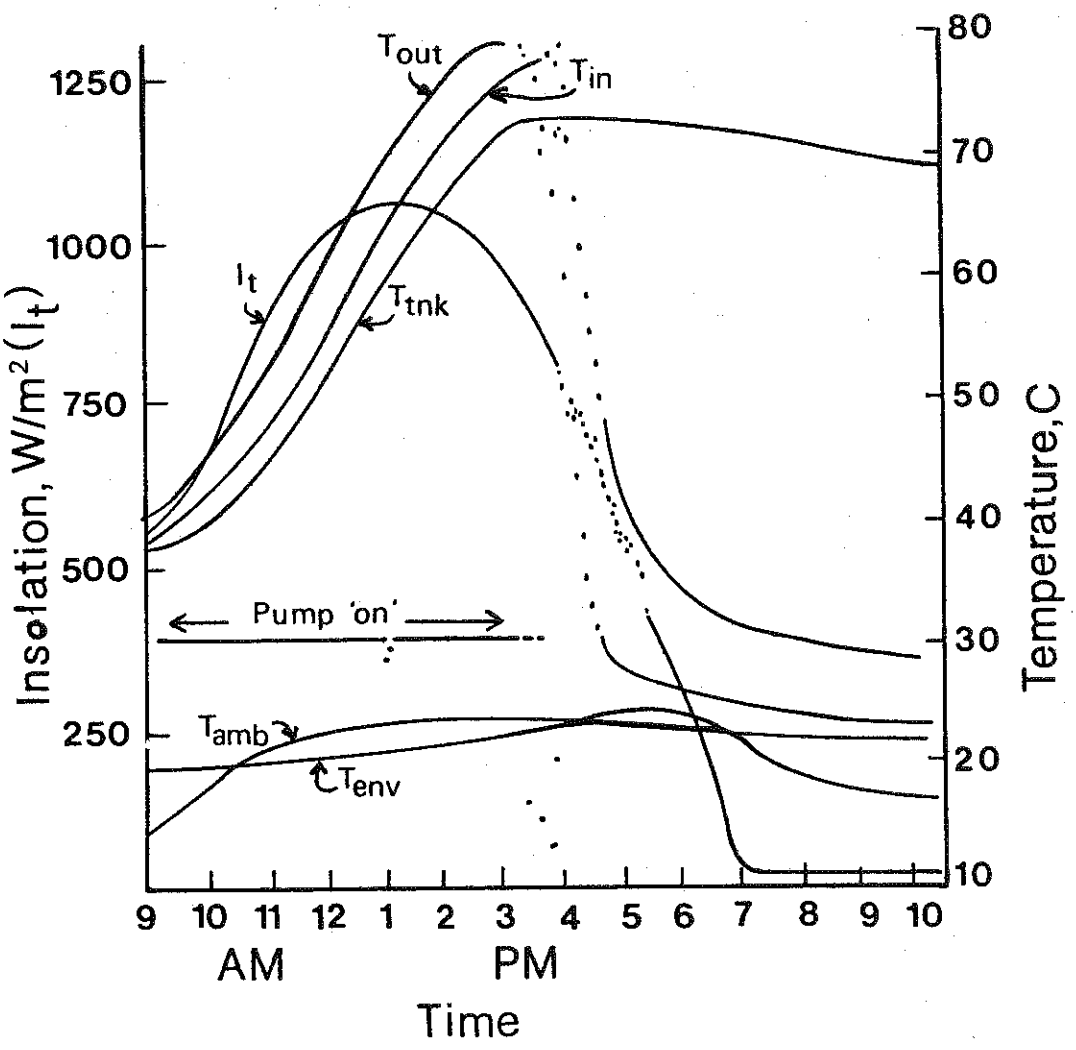

FIGURE 4.A.1. RAW DATA FROM MG&E SYSTEM TEST, SEPTEMBER 4, 1982.

m from the tank. The tank to ambient temperature difference varied between 19 C at the start of the day to 50 C at the time the circulating pump shut off. The analysis of section 3.B.3 implies that the error is about 10% of this temperature difference, giving an average error in sensed tank temperature of 3.5 C over the day.

The second problem in the system concerned the circulating pumps. The MG&E system, as mentioned previously, uses two pumps connected in series. This arrangement is necessary to provide sufficient head to raise the water the 7 m (23 feet) to the collectors on the roof.

Using published data on the Grundfos UP25-42SF pumps and estimates of pipe and collector pressure drops, the loop flow was estimated at between 0.20 and 0.25 l/s (3-4 gpm). This is far above the collector manufacturer's recommended flowrate of 0.06 to 0.12 l/s (0.5 to 1 gpm) for the two collectors.

The effect on the system of this high flow was to wipe out any tank stratification. In fact, when the DAS was first installed on the MG&E system, the collector loop inlet to outlet temperature difference was less than 1 C. Moreover, the collector loop inlet

temperature was 10-15 C higher than any measured tank temperature.

Given the internal construction of the tank, with a long (0.5 m) dip tube extending into the tank at the collector loop outlet connection, it is probable that the high flowrate was causing water to 'short-circuit' through the tank from the collector outlet to the pump inlet.

To decrease this effect, the outlet flange valve of the second pump in series was closed to about 30% of its wide-open position. This provided a higher collector temperature rise and brought the measured collector loop inlet temperature down to 3-4 C above the average tank temperature. The data plotted in Figure 4.A.1 were gathered after this adjustment was made.

The third problem encountered was not identified until the collector loop performance was plotted as in Figure 4.A.2. Each point in this figure represents 10 minute average values of efficiency and collector loop operating point. The time order of the points is indicated by the arrows connecting them. There is a clear pattern here, with lower efficiency for the same operating point in the beginning of the day than in the

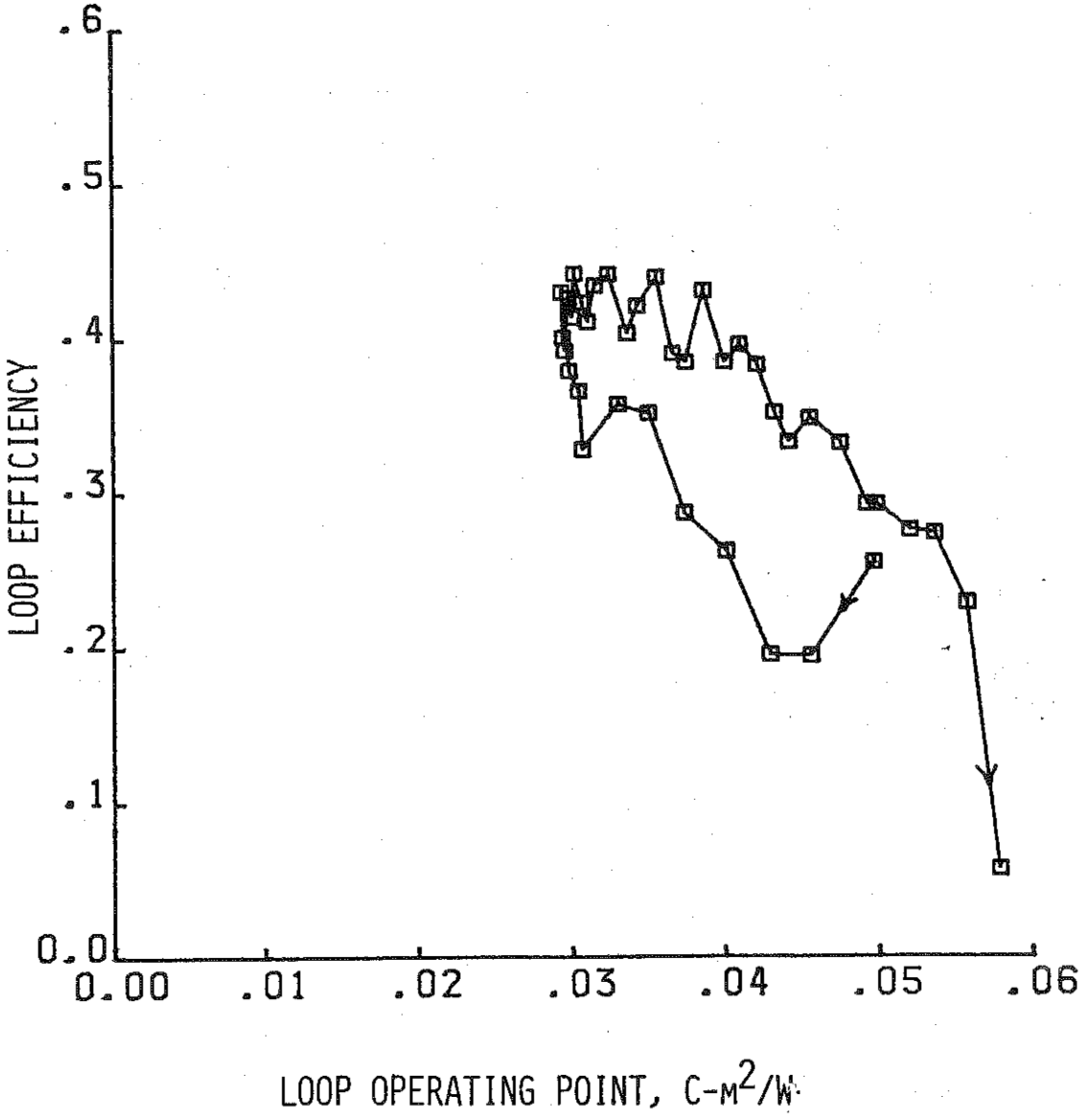

FIGURE 4.A.2. LOOP EFFICIENCY VS. OPERATING POINT FOR MG&E SYSTEM, SEPTEMBER 4, 1982. OBSERVATIONS ARE CONNECTED IN TIME ORDER.

latter part of the day.

The wide difference between morning and afternoon is due to the radiometer being mis-aligned, with its axis pointing more easterly than the collector plane. Collector surface insolation was over-estimated in the morning and under-estimated in the afternoon. This caused the morning estimates of efficiency to be biased low while the afternoon estimates were biased high.

The radiometer orientation was corrected by aligning the sensor plane with the collector plane using a long straight edge mounted on the radiometer and measuring the angle between it and the collector cover.

4.A.3. System Component Analysis

The data gathered during late September and October may be analyzed to find the solar storage tank loss coefficient, the circulator flowrate and the thermal efficiency of the collector loop.

4.A.3.a. Tank (UA) Value

The tank loss coefficient was calculated using 60 hours of tank temperature data starting in the evening of September 4 and running to the morning of September 7 (the 6th was a holiday). Since the 4th was a sunny

day, the average tank temperature was 71.3 C at the beginning of the period. By the end of 60 hours the tank had cooled to an average temperature of 48 C. The upper, middle and lower tank sensors differed by less than 2 C throughout the period, indicating little stratification. The room ambient temperature varied from a high of 22 C at the start of the test to 20 C at the end. The overnight minimum room temperature was 19.8 C at 4 AM on the 7th.

A linear regression on the data yielded a tank time constant of 100 hours. The 95% marginal confidence interval of this estimate is +/- 2 hours. For the tank volume of 310 l and assuming a thermal capacity of 4186 W-s/Kg-C and a density of 1 kg/l for water, the tank (UA) value is 3.6 (+/- 0.06) W/C (6.8 BTU/hr-F).

It is interesting to compare the experimental and calculated (UA) values. The tank has a surface area of 2.77 square meters and is insulated with a layer of chopped glass fiber 0.076 m (3 inches) thick. For tightly packed glass fiber, Krieth [34] gives a thermal conductivity of 0.038 W/m-C. These figures work out to a calculated (UA) of 1.38 W/C. This is less than half the experimental value.

The discrepancy between calculated and experimental (UA) comes as no surprise. The above calculation assumes a uniform layer of insulation covering the entire tank. However, there are several penetrations through the insulation for connection of piping. These penetrations allow heat to be lost directly from the small amount of tank shell exposed as well as providing, in the attached pipe, an extended surface for heat loss.

The large difference between calculated and experimental tank (UA) values has been noted by other researchers working under more closely controlled conditions [24].

4.A.3.b. Collector Loop Flowrate

The collector loop flowrate was found using the method described in Chapter 3. Data from September 22 and 23 were used. Figure 4.A.3 is a plot of this data on coordinates of loop energy gain vs temperature difference. A least squares line fitted to this data has a slope of 486 W/C (922 BTU/F-hr). This is equivalent to a flow of 0.12 l/s (1.84 gpm).

The collector manufacturer recommends a flow of 0.5 to 1 gallon per minute per module or 1 to 2 gpm for the array. The measured flowrate is within this range.

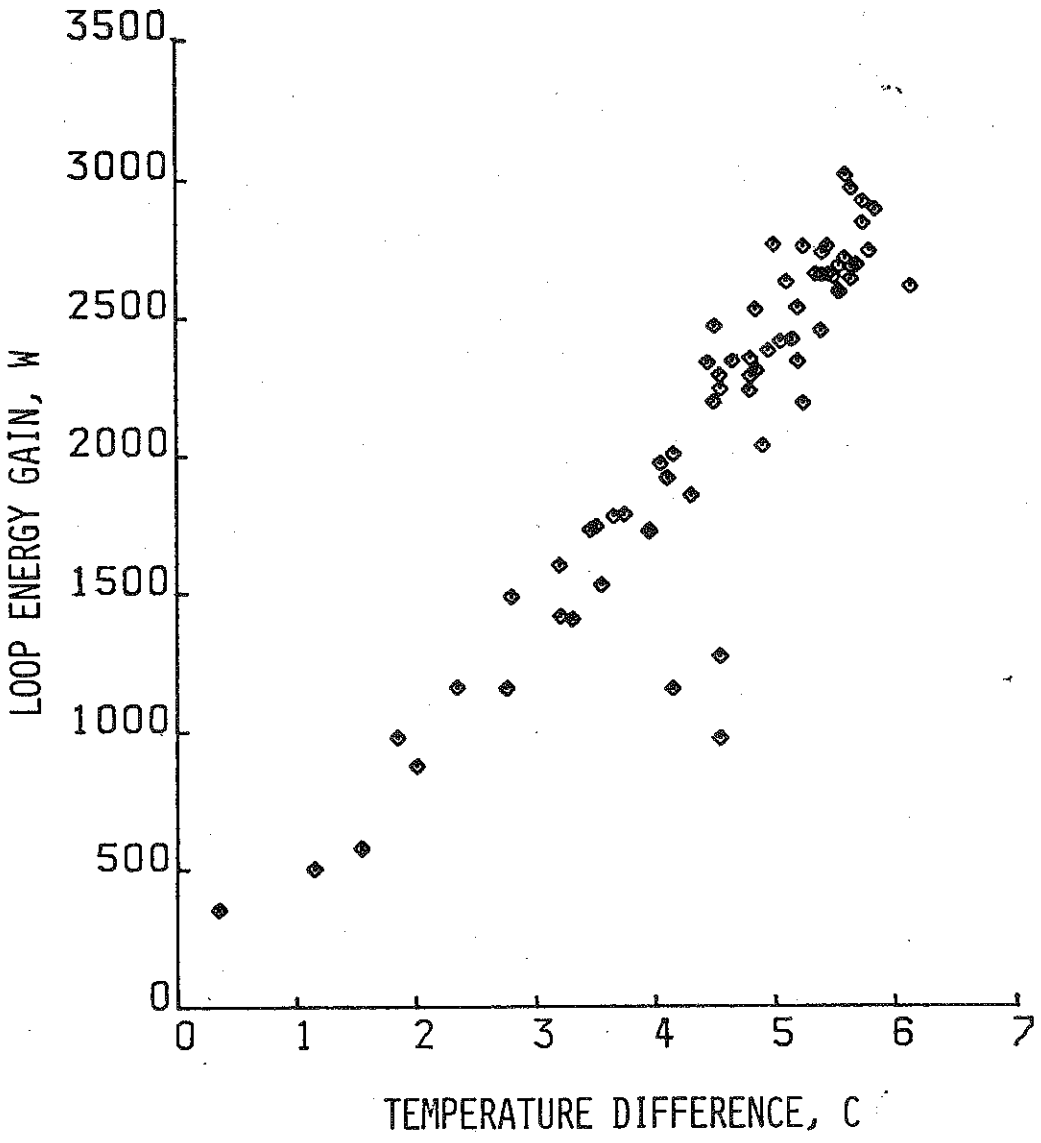

FIGURE 4.A.3. LOOP ENERGY GAIN VS COLLECTOR INLET TO OUTLET TEMPERATURE RISE, MG&E SYSTEM. DATA FROM SEPTEMBER 22 AND 23, 1982.

4.A.3.c. Collector Loop Performance

The collector loop performance was calculated from data gathered on October 15 and 16. Raw data for these days are plotted in Figure 4.A.4. The average tank temperature trace begins at a value of 25 C at 9 AM on the 15th. This test was started with a 'cold' tank after most of the hot water in the tank was drained and replaced with mains water. This allows a wider range of collector operating points during the test period.

As can be seen from Figure 4.A.4, the 15th was partly cloudly during the morning hours, with heavy cloud moving in between 1:30 and 3 PM, then clearing out between 3 and 4 PM. The circulator pumps were on from 9:15 AM to 1:30, with some short interruptions between 11 AM and 1 PM, denoted by the breaks in the 'pump on' trace in the plot.

The morning of the 16th was clearer, although the circulators started later than the previous day due to the higher initial tank temperature (48 C). The pumps were on steadily for about five hours, from 10 AM to 2 PM. After 2 PM some clouds moved in, resulting in erratic pump operation until around 3 PM, when the system shut down for the rest of the day.

Using the algorithms of Section 2.B, the data in

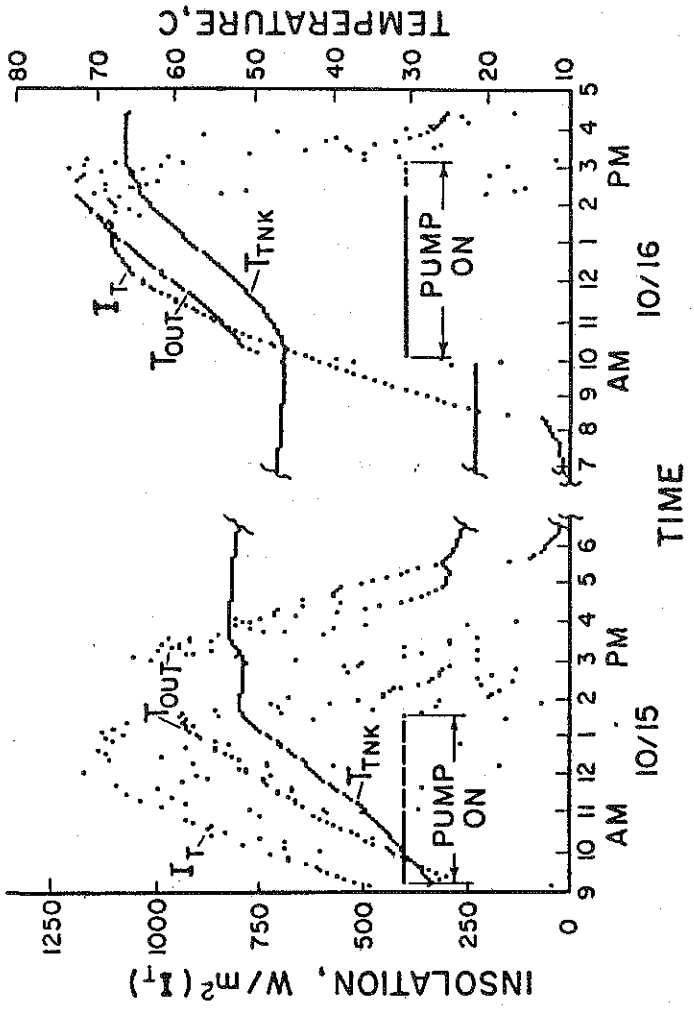

FIGURE 4.A.4. RAW DATA FROM MG&E SYSTEM TEST, OCTOBER 15 AND 16, 1982.

Figure 4.A.4 were reduced to the plot of Figure 4.A.5. The data fall into two distinct groups on this plot. The left group, representing a lower operating point, are from data gathered on the 15th. These points have more scatter than the right group, gathered on the next day. This scatter is due to the cloudy conditons holding on the 15th and the assumptions inherent in the data reduction algorithm.

The collector performance algorithm assumes that the system operates under steady state conditons over each data interval. Each point in figure 4.A.5 represents the average efficiency and operating point over a ten minute interval. If the sun is covered for part of the ten minute interval, the DAS will record less radiation for that interval although thermal capacitance effects in the collector and fluid will tend to smooth out the effects of rapid changes in insolation. In this case, the calculated efficiency and operating point will be greater than the true average over the interval.

Conversely, a sunny ten minute interval which follows a cloudy period will appear to have a lower efficiency, again due to thermal capacitance effects.

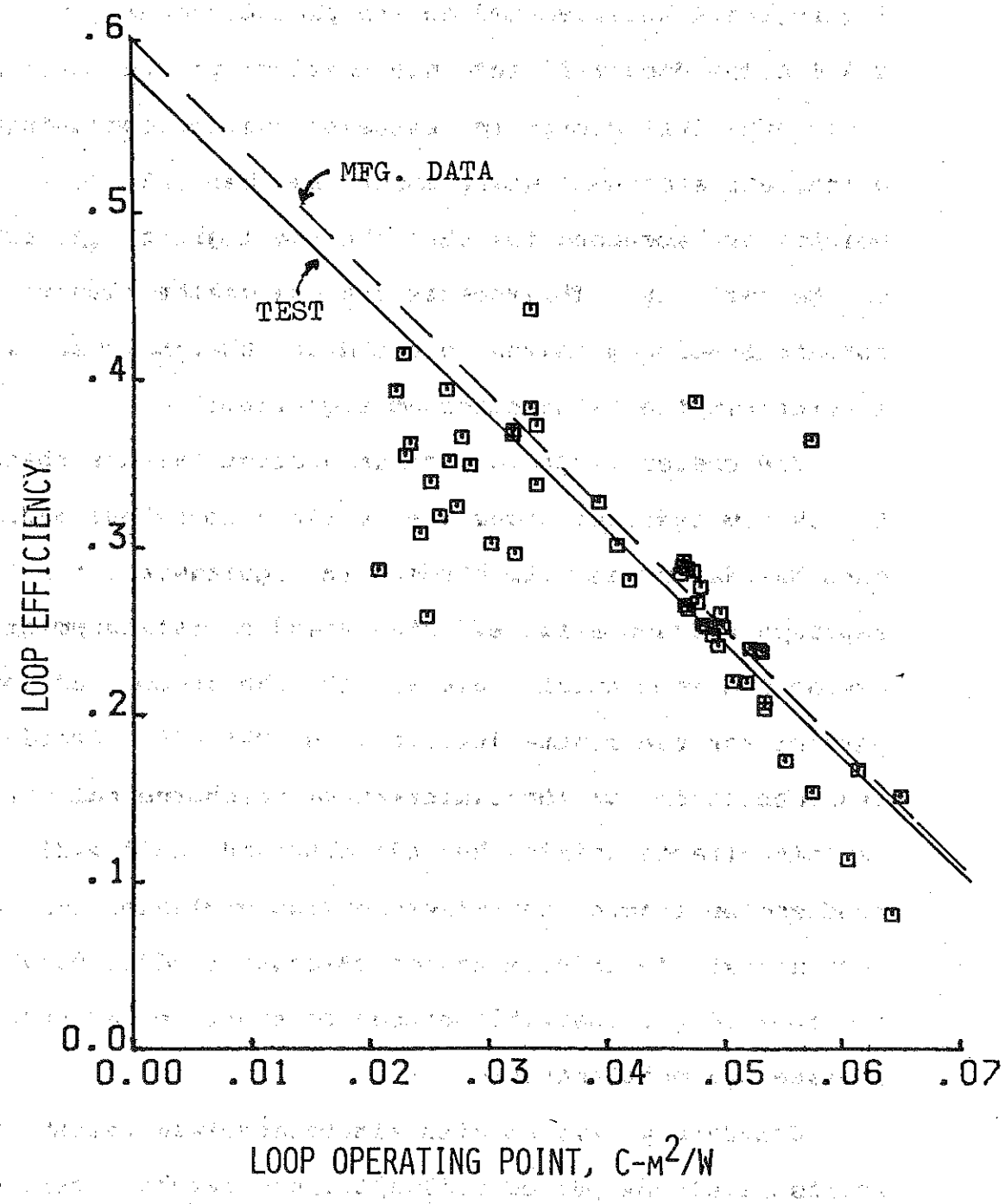

FIGURE 4.A.5. COLLECTOR LOOP EFFICIENCY VS. OPERATING POINT, MG&E SYSTEM, OCTOBER 15 AND 16, 1982.

Figure 4.A.6 is a time-order plot of the data from Figure 4.A.5. This plot shows that the scattered points of the 15th have no systematic bias due to the intermittent operating conditions.

A least-squares line fitted to the 82 data points in Figure 4.A.5 has a slope of 6.8 w/m^2-C (1.2 BTU/hr-ft^2) and an intercept of 0.58. The 95% marginal conficence limits are +/- 0.9 W/m^2-C on the slope and +/- 0.004 on the intercept. Collector loop performance is referenced to the gross area of the modules.

Manufacturer's data [35] for the collector alone give a slop of 5.9 w/m^2-C and an intercept of 0.61. The discrepancy between these and the measure values is due to two factors. First, the manufacturer's data is for normal incidence irradiation, while the test data cover a range of incident angles. Second, the collector loop includes 18 m of pipe covered with poor quality insulation. The effect of pipe losses on collector loop performance may be estimated using Equations 2.D.3 and 2.D.4. Using the measured flowrate and estimated inlet and outlet pipe (UA) values of 4.5 W/C (per pipe), the adjustment factors are:

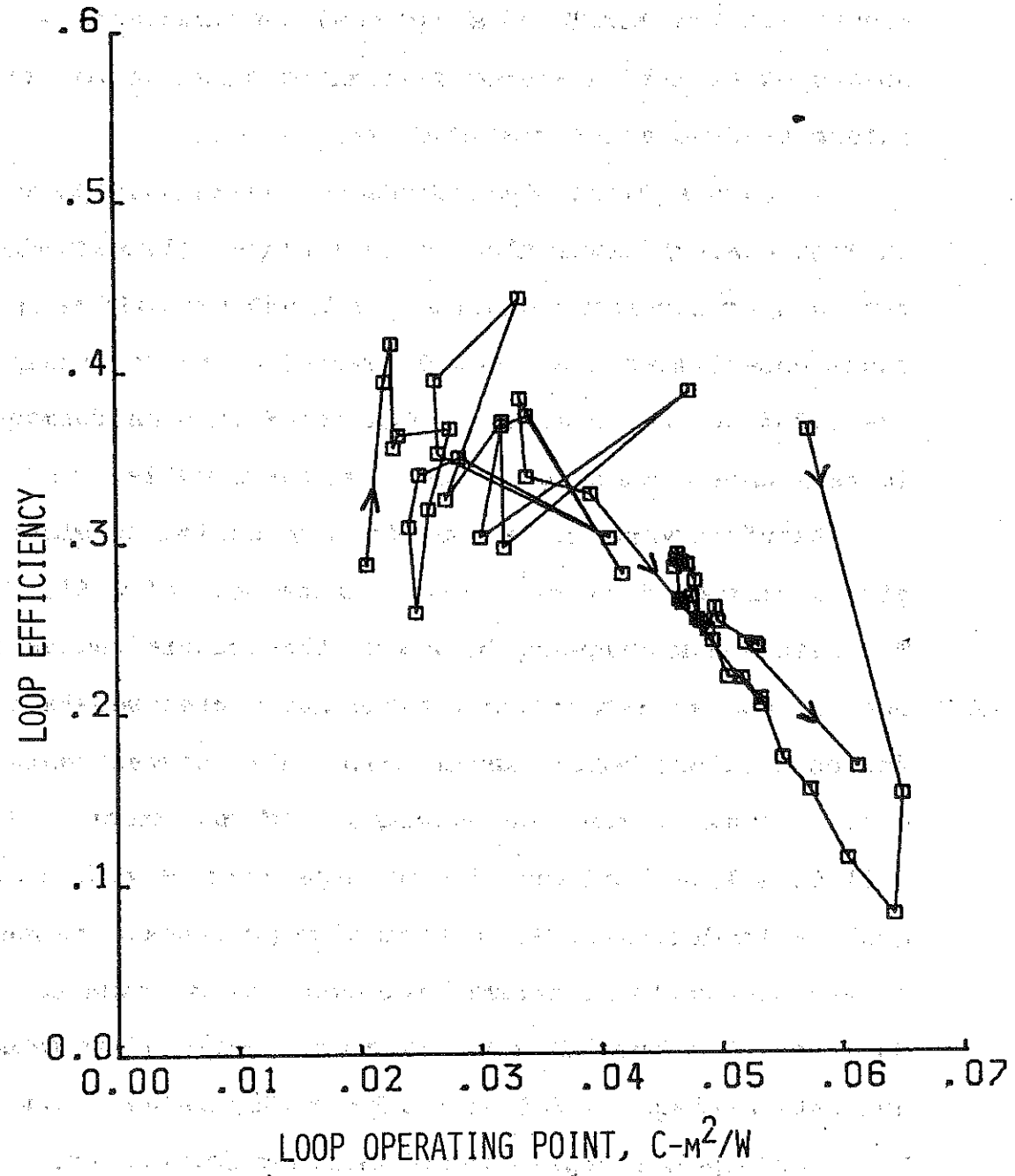

FIGURE 4.A.6. TIME ORDER OF LOOP EFFICIENCY VS. OPERATING POINT OBSERVATIONS, MG&E SYSTEM, OCTOBER 15 AND 16, 1982.

$$\frac{(\tau\alpha)'}{(\tau\alpha)} = 0.98$$

$$\frac{U_l'}{U_l} = 1.2$$

In SI units, the loop performance equations are:

Experimental: $\eta = 0.58 - 6.8\ (T_{in} - T_{amb})/I$

Mfg. w/pipe losses: $\eta = 0.60 - 7.0\ (Tin - Tamb)/I$

These lines are plotted on Figure 4.A.7.

4.A.4. Extrapolation of Long Term Performance

The long term performance of the MG&E SDHW system can be predicted using the $\bar{\phi}$, f-Chart design method outlined in Section 1.D.

The parameters used are listed in Table 4.A.1. The values in the table are classified as to their source: measured, calculated or estimated. Measured values, such as collector area, were taken directly from system components. Calculated values, such as tank insulation conductance, were developed from test data. Some values, such as auxiliary tank (UA), were estimated.

Table 4.A.2 presents values of long term annual average solar fraction. These values were calculated using parameters derived from the system tests and listed in Table 4.A.1. The range of set temperature

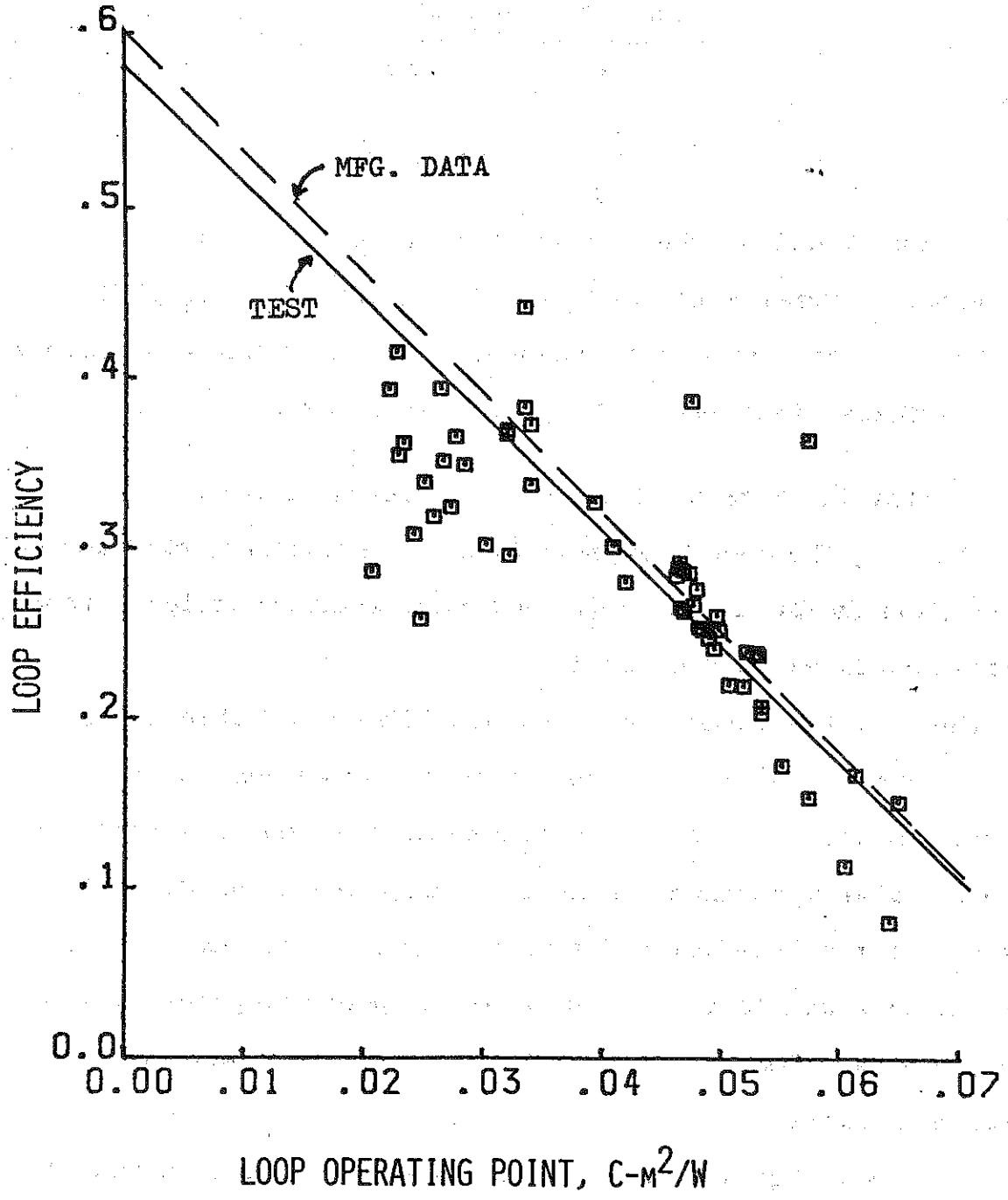

FIGURE 4.A.7. COLLECTOR LOOP EFFICIENCY VS. OPERATING POINT, MG&E SYSTEM, OCTOBER 15 AND 16, 1982.

and daily load volumes listed in the table represent different operating conditions for the system.

Parameters Used in FCHART Runs

Parameter	Value	Source
Collector area	7.1 m^2	measured
$F_r U_l$	6.8 W/m^2-C	calculated
$F_r (\tau\alpha)$	0.58	calculated
Incident angle modifer constant	0.01	(see text)
Collector slope	45 deg	measured
Collector azimuth	-10 deg	measured
Ground reflectance	0.2	estimated
Tank capacity/ collector area	183 kJ/m^2-C	calculated
Tank height/diameter	2.56	measured
Tank 'U'	1.28 W/m^2-C	calculated
Environment temperature	20 C	estimated
Auxiliary tank (UA)	3.23 W/C	estimated
Auxiliary tank env.	20 C	estimated
Auxiliary fuel	nat. gas	--
Auxiliary firing eff.	60%	estimated

Table 4.A.1. Parameters used in FCHART runs for MG&E system.

Results of FCHART Runs

Set Temp., C	40	50	60
	0.72	0.57	0.47
	0.59	0.46	0.37
	0.50	0.38	0.31
	0.43	0.33	0.27

Estimated values of long term annual
fraction for various daily load and set
alues. Mains temperature fixed at 11 C.

r fractions generated by FCHART 4.2 are

$$- \frac{Q_{aux}}{Q_{load} + Q_{loss}} \qquad (4.A.1)$$

uxiliary energy delivered to the hot
is the energy removed from the system in
ot water and Q_{loss} is the energy lost from
auxiliary storage tanks.

hased auxiliary energy is greater than
he less-than-unity firing efficiency of
iary heater, estimated at 60% for this
rchased energy required to operate a
DHW system consisting of the auxiliary
given by:

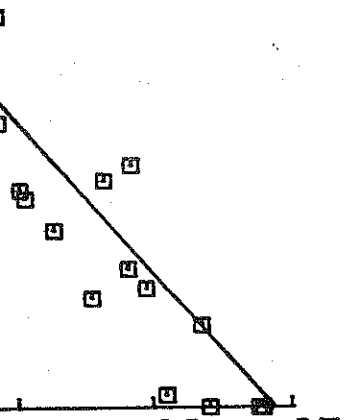

2/W

NCY VS.

8 AND 9, 1983.

$$\frac{(\tau\ \alpha)'}{(\tau\ \alpha)} = 0.99$$

$$\frac{Ul'}{Ul} = 1.14$$

$$\frac{Fr'}{Fr} = 0.80$$

The first order collector loop performance equation, in SI units, becomes:

$$eff = 0.59 - 4.2\ \Delta T/I$$

The intercept of this equation is reasonable close to the measured intercept of 0.55 (+/- 0.02) but the slope is only about half the measured value of 8.1 W/m^2-C (+/- 0.6).

The discrepancy between measured and calculated loop performance may be due to many causes. Among these are measurement errors, collector degradation, poor flow distribution between collectors in parallel and deteriorated pipe insulation.

Gross measurement errors are an unlikely culprit, since the previous test of the MG&E system gave good agreement between test results and manufacturer's data.

The effects of collector degradation are difficult to quantify. The two most likely problem areas are the selective absorber surface and the integrity of the

collector enclosure. Degradation of the selective properties of the absorber would tend to increase the collector loss coefficient. Moisture entering the enclosure would also increase collector losses.

The effects of collector degradation are difficult to quantify. The two most likely problem areas are the selective absorber surface and the integrity of the collector enclosure. Degradation of the selective properties of the absorber would tend to increase the collector loss coefficient. Moisture entering the enclosure would also increase collector losses.

The effect of changes in pipe insulation conductivity are more easily quantified. A doubling of insulation conductivity to 0.042 W/m-C would result in the correction factors:

$$\frac{(\tau\ \alpha)'}{(\tau\ \alpha)} = 0.99 \qquad \frac{Ul'}{Ul} = 1.27$$

The loop performance equation becomes:

$$eff = 0.57 - 4.5\ \Delta T/I$$

The effect of doubling the pipe loss estimate is not great. By a process of elimination, it appears

that some collector degradation has occurred, although the extent and nature of the changes are difficult to determine.

4.B.3. Estimation of Long Term Performance

The long term performance of the system was estimated with the same methodology used for the previous system. The FCHART 4.1 parameters used are presented in Table 4.B.1.

Table 4.B.2 presents values of long term annual average solar fraction for several different combinations of set temperature and water usage.

Estimates of the system's purchased energy savings are presented in Table 4.B.3.

Parameters Used in FCHART Runs
Beckman System

Parameter	Value	Source
Collector area	4.2 m^2	measured
F_rU_l product	8.1 W/m^2-C	calculated
$F_r(\tau\alpha)$	0.55	calculated
Incident angle modifier constant	0.01	(see text)
Collector slope	45 deg	measured
Collector azimuth	0 deg	measured
Ground reflectance	0.2	estimated
Tank capacity/ collector area	309 KJ/m^2-C	calculated
Tank height/diameter	2.6	measured
Tank 'U'	1.7 W/m^2-C	calculated
Environment temperature	20 C	estimated
Auxiliary tank (UA)	3.23 W/C	estimated
Auxiliary tank env.	20 C	estimated
Auxiliary fuel	nat. gas	--
Auxiliary firing eff.	60%	estimated

Table 4.B.1. Parameters used in FCHART runs for Beckman system.

Results of FCHART Runs
Beckman System

Set Temp. C	40	50	60
Load l/day			
150	0.52	0.40	0.32
300	0.41	0.31	0.25
450	0.34	0.25	0.28
600	0.29	0.22	0.17

Table 4.B.2 Estimated values of long term annual average solar fraction for various daily load and set temperature values. Mains temperature fixed at 11 C.

Beckman System Purchased Energy Requirements
GJ/Year

Load, l/day \ Set Temp. C	40	50	60
150	7.6	7.9	8.1
300	10.5	10.8	11.0
450	12.5	12.6	12.8
600	13.9	14.0	14.1

Table 4.B.3. Estimated values of long term average annual purchased energy savings for variuos daily load and set temperature values. Mains temperature fixed at 11 C.

4.B.4. Evaluation of System Modifications

The Beckman SDHW system performance, as estimated above, is very poor. Performance could be improved by replacing the existing in-tank heat exchanger, which has a measured effectiveness of 0.21, with an external counterflow unit. Published data on counterflow heat exchangers for solar applications claim an effectiveness of 0.5 and greater. This would be a major modification of the system and should not be undertaken unless some estimate of its benefit can be make.

A higher effectiveness heat exchanger would increase the effective heat removal factor of the

system, F_r'. This factor is defined in terms of other system parameters:

$$\frac{F_r'}{F_r} = \left(1+ \frac{A_c F_r U_l'}{(\dot{m}C_p)_c} (1/\varepsilon - 1)\right)^{-1} \qquad (4.B.1)$$

A_c is the collector area, $F_r U_l'$ is the product of the heat removal factor and the pipe loss-adjusted collector loss coefficient, $(\dot{m}C_p)_c$ is the collector capacitance rate and ε is the heat exchanger effectiveness.

The collector area, capacitance rate and heat exchanger effectiveness have been measured. The $F_r U_l'$ product of the actual collector can be estimated by solving Equation 4.B.1 for the $F_r U_l$ product of the collector, estimated to be 9.9 $W.m^2$-C. The value of the heat exchanger factor for present collector-heat exchanger combination, with a heat exchanger effectiveness of 0.21, can be calculated from equation 4.B.1 and is 0.67. The collector-heat exchanger combination with an effectiveness of 0.5 has a F_r'/F_r ratio of 0.87. The ratio of these two values (0.87/0.67 = 1.38) can be used to calculate a new set of collector parameters:

$$F_r'U_l' = 10.5\ W/m^2\text{-}C;\ F_r'(\tau\alpha)' = 0.72$$

These collector parameters can be used in another set of FCHART 4.1 runs to estimate the change in purchased energy use between the existing system and the system with the higher performance heat exchanger. The results of these runs are summarized in Table 4.B.4.

As can be seen in Table 4.B.4, this system modification results in a decrease in purchased energy demand. At the current cost of natural gas, the maximum savings would be around $20/year, perhaps not enough to justify the cost of the new heat exchanger.

Decrease in Beckman System Purchased Energy Requirements

	GJ/Year		
Set Temp. C	40	50	60
Load l/day			
150	1.0	1.2	1.2
300	1.6	1.7	1.7
450	2.0	2.2	2.2
600	2.5	2.5	2.6

Table 4.B.4. Estimated decrease in purchased energy required by Beckman system after replacement of existing heat exchanger with a unit with effectivness = 0.5. Mains temperature fixed at 11 C.

Chapter 5

Summary

The methodology described in the previous chapters is suitable for the in situ testing of most SDHW systems in use today. This includes those with single and double tank storage and those using direct and indirect collector to storage transfer.

The system parameters needed to use the $\overline{\phi}$, f-Chart design method can be measured by this test. The method is also suitable for measuring heat exchanger effectiveness and pump flowrates, both useful diagonostic values.

The test method can be implemented in low-cost hardware using mostly off-the-shelf components.

An existing SDHW system needs minimal modification in order to be tested. During testing, a two tank system can continue to provide hot water from its auxiliary tank.

At least two days of relatively clear weather are needed to develop adequate operating data.

The test method can be extended to larger systems by use of more temperature sensors.

Several areas for future study are obvious.

First, the testing methodology should be verified by using it to analyze data gathered from a more extensively instrumented system such as one of the systems constructed at the NBS test facility in Gaithersburg, Maryland.

Second, the accuracy of the simple DAS constructed for this project could be checked, perhaps by using it side-by-side with the NBS test sytems mentioned above.

Several refinements to the DAS are desirable. These include using a battery operated portable computer in place of the Apple II and bubble memory in place of the floppy disk.

The system software could be upgraded in several areas. Higher speed and more on-line data reduction could be acheived by converting much of the data reduction software to assembly code or using a compiled language in place of Applesoft BASIC.

Finally, the testing methodology could be extended to other solar thermal systms, including space heating systems and systems using air heating collectors. Thermosyphon and 'breadbox' type solar water heaters are also appropriate candidates for short term testing. Thermosyphon systems could perhaps be tested if the loop flow status could be monitored.

Bibliography

1. Duffie, J. A. and Beckman, W. A., Solar Engineering of Thermal Processes, Wiley-Interscience, New York (1980).

2. Buckles, W. E., and Klein, S. A., "Analysis of Solar Water Heaters', Solar Energy, 25, 417 (1980).

3. Daniels, F., Direct Use of the Sun's Energy, Yale University Press, (1964).

4. Hottlel H. C., and Whillier, A., 'Evaluation of Flat Plate Collector Performance', Transactions of the Conference on the Use of Solar Energy, 2, Part I, 74, University of Arizona Press (1958).

5. ASHRAE, Standard 93-1977, 'Methods of Testing to Determine the Performance of Solar Collectors', American Society of Heating, Refrigeration and Air Conditioning Engineers, New York (1977).

6. deWinter, F., 'Heat Exchanger Penalties in Double-Loop Solar Water Heating Systems', Solar Energy, 17, 335 (1975).

7. Winn, C. B., and D. E. Hull, 'Optimal Controllers of the Second Kind', Proceedings of the 1978 Annual Meeting of the AS of ISES, Denver, 2(2), 493 (1978).

8. Liu, B. Y. H., and Jordan, R. C., 'The Inter-relationship and Characteristic Distribution of Direct, Diffuse and Total Solar Radiation', Solar Energy, 4(3), (1960).

9. Erbs, D. G., Klein, S. A., and Duffie, J. A., 'Estimation of Diffuse Radiation Fraction for Hourly, Daily and Monthly-Average Global Radiation', Solar Energy, 24, 293, (1982).

10. Klein, S. A. and Beckman, W. A., 'A General Design Method for Closed-Loop Solar Energy Systems', Solar Energy, 22, 269, (1979).

11. Hourly Solar Radiation-Surface Meteorological Observations, SOLMET Volume II Users Manual, US Department of Commerce, NOAA, Asheville, North

Carolina (1979).

12. Liu, B. Y. H. and Jordan R. C., 'The Long-Term Average Performance of Flat-Plate Solar Energy Collectors', Solar Energy, 7(53), (1963).

13. Klein, S. A., Beckman, W. A. and Duffie, J. A., 'A Design Procedure for Solar Heating Systems', Solar Energy, 18, (113), (1976).

14. Duffie, J. A. and Mitchell, J. W., 'f-Chart: Predictions and Measurements', Journal of Solar Energy Engineering, 105(3), (1983).

15. FCHART 4.1, University of Wisconsin Engineering Experiment Report 50, (1982).

16. Clark, D. R., Klein, S. A. and Beckman, W. A., 'An Algorithm for Evaluating the Hourly Utilizability Function', Journal of Solar Energy Engineering, in press.

17. Braun, J. E., Klein, S. A., and K. A. Pearson, 'An Improved Design Method for Solar Water Heating System', Solar Energy, in press.

18. Fanney, A. H. and Liu, S. T., 'Comparison of Experimental and Computer-Predicted Performance for Six Solar Domestic Hot Water Systems', ASHRAE Transaction, 86, I, pp. 393-402 (1980).

19. Chandra, S. and Khatter, M. K., 'Analytical Investigations of the Relative Solar Rating Concept', Florida Solar Energy Center Report FSEC-TT-80-6 (1980).

20. Morgan, R., 'The Wisconsin Power and Light Company Residential Solar Domestic Water Heating Program Performance Report', Wisconsin Power and Light Company Consumer Services Department (1982).

21. Odegard, D. S. and Penfield, D., 'Northeast Solar Domestic Hot Water Performance Monitoring', Proceedings of the ASME Solar Energy Conference, Albuquerque, New Mexico (1982).

22. August, W. K., 'Preliminary Results-SDHW Monitioring in Pennsylvania', Conference

Proceedings-Solar Heating and Cooling Systems Operational Results, Solar Energy Research Institue, SERI/TP-245-430, Golden, Colorado (1979).

23. Cramer, M. A., Spears, J. W. and Pollock, E. O, Comparative Report: Performance of Solar Hot Water Systems 1980-1981, National Solar Data Network, NTIS SOLAR/0024-82/41.

24. Fanney, A. H., 'Analytical and Experimental Analysis of Procedures for Testing Solar Domestic Hot Water Sytems', PhD Thesis, Virigina Polytechnic Institute (1981).

25. Klein, S. A. and Fanney, A. H. 'A Rating Procedure for Solar Domestic Water Heating Systems', ASME Journal of Solar Energy Engineering, in press.

26. Mutch, J. J., 'Residential Water Heating: Fuel Conservation, Economics and Public Policy', Rand Corporation, R-1498-NSF (1974).

27. Knapp, C. L., Stoffel, T. L. and Whitaker, S. D., Insolation Data Manual, Solar Energy, Research Institute, Golden, Colorado (1980).

28. Feiereisen, T. J., 'An Experimental Study of Immersed Coil Heat Exchangers', M.S. Thesis, University of Wisconsin-Madison (1982).

29. TRNSYS Version 11.1, University of Wisconsin Engineering Experiment Station Report 38-11 (1981).

30. Box, G. E. P., Hunter, W. G. and Hunter, J. S., Statistics for Experimenters, Wiley, New York, NY (1978).

31. Worth, D. and Lechner, P., Beneath Apple DOS, Quality Software, Reseda, CA (1981).

32. Ohte, A. and Yamagata, M., 'A Precision Silicon Transistor Thermometer', IEEE Transactions on Instrumentation and Measurements, IM-26 (4) pp. 335-341 (1977).

33. MC6840 Programmable Timer Module, Product Data Sheet, Motorola Inc., Phoenix, AZ (1977).

34. Krieth, F., Principles of Heat Transfer, 3rd edition, Intext, New York, NY (1976).

35. Hundt, R., Lennox, Inc. Research and Development Laboratory, Carrollton, TX, personal communication.

36. Solar Products Specification Guide, p. 178, SolarVision, Inc. Harrisville, NH (1982).

Appendix A

Calculation of Marginal Confidence Intervals

The development outlined here follows that presented in Reference (30), Chapter 14. The calculation demonstrated is for the collector loop efficiency, but the same procedure was used to find confidence intervals for the other calculated values.

For the collector efficiency equation, the model is:

$$= F_r'(\tau\alpha)' - F_r'U_l'(T_{in}-T_{amb})/I_t \qquad (A.1)$$

For simplicity, this may be re-written as:

$$y = a + b\,x \qquad (A.2)$$

y represents , the loop efficiency, a represents $F_r'(\tau\alpha)'$, the loop intercept efficiency, b is $F_r'U_l'$, the product of the collector heat removal factor and overall loss coefficient and x is $(T_{in}-T_{amb})/I_t$, the loop operating point.

System test data is used to calculate y and x for each ten-minute period of pump operation. The

resulting values are used to estimate the 'best' values of a and b using the equations:

$$b = \frac{n\ \Sigma xy - \Sigma x\ \Sigma y}{n\ \Sigma x^2 - (\Sigma x)^2} \qquad (A.3)$$

$$a = \frac{\Sigma x^2\ \Sigma y - \Sigma x\ \Sigma xy}{n\Sigma x^2 - (\Sigma x)^2} \qquad (A.4)$$

n is the number of observations o x and y.

The residual sum of squares, S_r, is:

$$S_r = \Sigma xy + b\Sigma x^2 + 2ab\Sigma x - 2b\Sigma xy - 2a\Sigma y + 2a^2 n \qquad (A.5)$$

On the assumption that the model adequately fits the data, the error variance, S^2 is:

$$S^2 = \frac{S_r}{n-2} \qquad (A.6)$$

The standard errors of a and b are then:

$$S.E.(a) = \left(\frac{S^2/n}{(1-r^2)}\right)^{1/2} \qquad (A.7)$$

$$S.E.(b) = \left(\frac{S^2/\Sigma x^2}{(1-r^2)}\right)^{1/2} \qquad (A.8)$$

Where:

$$r^2 = \frac{(\Sigma x)^2}{n\Sigma x^2} \qquad (A.9)$$

The mariginal 95% confidence intervals are:

for a: a +/- (S.E.(a) * t)

for b: B +/- (S.E.(b) * t)

Where t is the point of the Student's t distribution that correpsonds to n-2 degrees of freedom and leaves a 0.025 tail area.

APPENDIX B

SOFTWARE LISTINGS

B.1 Executive Module

```
                    1010 ;       TEMPERATURE SENSOR
                    1020 ;       SCANNER PROGRAN
                    1030 ;
                    1040 ;       WARREN BUCKLES
                    1050 ;       1/26/82
                    1060 ;
                    1070 ; VARIABLES USED:
                    1080 ;   CHCNT--CHANNEL COUNTER (0-7)
                    1090 ;   CHTAB--BASE ADDRESS OF CHANNEL
                    1100 ;           ENABLE TABLE
                    1110 ;   ACNT--AUTO-RANGE COUNTER
                    1120 ;   ALIM--AUTO-RANGE ITERATION
                    1130 ;         LIMIT
                    1140 ;   INBASE--BASE ADRESS OF INPUT
                    1150 ;           CHANNELS ($C080+16X3+8)
                    1160 ;   LOLIM--AUTO RANGE LOW LIMIT
                    1170 ;   HILIM--AUTO RANGE HI LIMIT
                    1180 ;   ARBYTE--INDICATOR OF AUTO
                    1190 ;           RANGE OPERATION
                    1200 ;   RBASE--BASE OF RANGE TABLE
                    1210 ;   TBASE--BASE OF TOTAL TABLE
                    1220 ;   TBASE1--BASE OF TT HI BYTE
                    1230 ;
C0B8-               1240 INBASE .EQ $C080+$38
C0B0-               1250 CBASE  .EQ INBASE-8
0001-               1255 RSTCMD .EQ $01       ;PTM RESET
0004-               1260 CH3MSK .EQ $04
0002-               1270 CH2MSK .EQ $02       ;CHANNEL 2 INT
0001-               1280 CH1MSK .EQ $01       ;CHANNEL 1 INT
C0A1-               1290 STATUS .EQ $C0A1     ;PTM STATUS LOC
C0A0-               1295 CMDLOC .EQ $C0A0     ;PTM COMMAND LOC
FF3F-               1300 IOREST .EQ $FF3F
FF4A-               1310 IOSAVE .EQ $FF4A
                    1320        .OR $9B00
                    1330        .TF MAIN-INT-9B00.OBJ
9B00- A9 00         1340 TSCAN  LDA #$0
9B02- AA            1350        TAX
9B03- A9 00         1360 STORE1 LDA #$0
9B05- 9D B8 9B      1370        STA TBASE,X  ;ZERO OUT
9B08- 9D C0 9B      1380        STA TBASE1,X ;TOTAL REGS
9B0B- E8            1390        INX
```

```
9B0C- 8A        1400          TXA
9B0D- C9 08     1410          CMP #$08
9B0F- D0 F2     1420          BNE STORE1
9B11- A9 00     1430          LDA #$0
9B13- AA        1440          TAX
9B14- A9 FF     1450 STORE2   LDA #$FF
9B16- 9D B0 C0  1460          STA CBASE,X   ;SET UP CURRENT
9B19- E8        1470          INX
9B1A- 8A        1480          TXA
9B1B- C9 08     1490          CMP #$08
9B1D- D0 F5     1500          BNE STORE2
9B1F- A9 FF     1510          LDA #$FF      ;SET UP COUNTER
9B21- 8D A5 9B  1520          STA CHCNT     ;SAVE IT
9B24- EE A5 9B  1530 LOOP1    INC CHCNT     ;INC COUNTER
9B27- AD A5 9B  1540          LDA CHCNT     ;GET COUNTER
9B2A- C9 08     1550          CMP #$08      ;END OF SCAN?
9B2C- F0 72     1560          BEQ ESCAN     ;ALL DONE
9B2E- AA        1570          TAX           ;X PTS. TO CHANNEL
9B2F- A9 00     1580          LDA #$0       ;CHECK FOR
9B31- DD A8 9B  1590          CMP CHTAB,X   ;ACTIVE CHANNEL
9B34- F0 EE     1600          BEQ LOOP1     ;SKIP IF NOT
9B36- 8D A6 9B  1610          STA ACNT      ;INIT A-R CTR
9B39- BD B8 C0  1620 READ1    LDA INBASE,X  ;READ ADC
9B3C- EA        1630          NOP           ;WAIT
9B3D- EA        1640          NOP           ;A
9B3E- EA        1650          NOP           ;WHILE
9B3F- EA        1660          NOP
9B40- EA        1670          NOP
9B41- BD B8 C0  1680          LDA INBASE,X  ;REAL READ
9B44- CD A1 9B  1690          CMP LOLIM     ;CHECK FOR
9B47- B0 19     1700          BCS CHKHI     ;UNDER RANGE
9B49- FE B0 9B  1710          INC RBASE,X   ;CRANK IT UP
9B4C- BD B0 9B  1720          LDA RBASE,X   ;GET RANGE
9B4F- 9D B8 C0  1730          STA INBASE,X  ;SET IT
9B52- EE A6 9B  1740          INC ACNT      ;INCREMENT
9B55- AD A3 9B  1750          LDA ALIM      ;AND CHECK
9B58- CD A6 9B  1760          CMP ACNT      ;COUNTER
9B5B- 8D A7 9B  1770          STA ARBYTE    ;SHOW CHANGE
9B5E- F0 C4     1780          BEQ LOOP1     ;FINALLY BRANCH
9B60- D0 D7     1790          BNE READ1     ;OR ELSE
                1800 *                      ;RE READ
9B62- CD A2 9B  1810 CHKHI    CMP HILIM     ;CHECK FOR
9B65- 90 19     1820          BCC LOOP2     ;HI OVERRANGE
9B67- DE B0 9B  1830          DEC RBASE,X
9B6A- BD B0 9B  1840          LDA RBASE,X   ;SAME AS ABOVE
9B6D- 9D B8 C0  1850          STA INBASE,X
9B70- EE A6 9B  1860          INC ACNT
9B73- AD A3 9B  1870          LDA ALIM
9B76- CD A6 9B  1880          CMP ACNT
```

```
9B79- 8D A7 9B 1890          STA ARBYTE
9B7C- F0 A6    1900          BEQ LOOP1
9B7E- D0 B9    1910          BNE READ1
9B80- BD B8 C0 1920 LOOP2    LDA INBASE,X ;READ CHANNEL
9B83- AD A4 9B 1930          LDA SCNT     ;PICK UP SCAN
9B86- A8       1940          TAY          ;WHILE WAITING
9B87- EA       1950          NOP
9B88- 18       1960 READ2    CLC          ;SET UP ADD
9B89- BD B8 C0 1970          LDA INBASE,X ;READ IT AGAIN
9B8C- 7D B8 9B 1980          ADC TBASE,X  ;KEEP SUM
9B8F- 9D B8 9B 1990          STA TBASE,X  ;OF READINGS
9B92- 90 03    2000          BCC LCHK     ;IN 2 BYTES
9B94- FE C0 9B 2010          INC TBASE1,X ;
9B97- 88       2020 LCHK     DEY          ;DEC AND
9B98- 98       2030          TYA
9B99- C9 00    2040          CMP #$0      ;CHECK COUNTER
9B9B- D0 EB    2050          BNE READ2    ;READ IT AGAIN
9B9D- 4C 24 9B 2060          JMP LOOP1    ;OR GO TO NEXT
9BA0- 60       2070 ESCAN    RTS
               2080 ;
               2090 ;        START OF DATA AREA
               2100 ;
9BA1- 20       2110 LOLIM    .DA #$20
9BA2- E0       2120 HILIM    .DA #$E0
9BA3- 80       2130 ALIM     .DA #$80
9BA4- 0A       2140 SCNT     .DA #$0A
9BA5-          2150 CHCNT    .BS 1
9BA6-          2160 ACNT     .BS 1
9BA7-          2170 ARBYTE   .BS 1
9BA8-          2180 CHTAB    .BS 8
9BB0-          2190 RBASE    .BS 8
9BB8-          2200 TBASE    .BS 8
9BC0-          2210 TBASE1   .BS 8
               2220 ;
               2230 ;  BEGINNING OF INTERRUPT HANDLER
               2240 ;
9BC8- 78       2250 SERV     SEI          ;DISABLE INTERRUPTS
9BC9- A5 45    2260          LDA $45      ;RESTORE ACC
9BCB- 20 4A FF 2270          JSR IOSAVE   ;SAVE CPU REGS
9BCE- AD A1 C0 2280          LDA STATUS   ;GET PCM STAT
9BD1- 29 04    2350          AND #CH3MSK  ;DETERMINE
9BD3- F0 03    2360          BEQ CH2TST   ;SOURCE OF INT
9BD5- 20 F4 9B 2370          JSR TICK     ;AND DO IT
9BD8- AD A1 C0 2380 CH2TST   LDA STATUS   ;STATUS AGAIN
9BDB- 29 02    2390          AND #CH2MSK  ;IS IT THE
9BDD- F0 03    2400          BEQ CH1TST   ;PUMP?
9BDF- 20 3E 9C 2410          JSR PUMP     ;DO PUMP
9BE2- AD A1 C0 2420 CH1TST   LDA STATUS   ;MORE STAT
9BE5- 29 01    2430          AND #CH1MSK  ;IS IT RAD
```

```
9BE7- F0 03     2440          BEQ DONE       ;OR ARE WE DONE?
9BE9- 20 48 9C  2450          JSR RAD        ;DO RAD
9BEC- 20 3F FF  2460 DONE     JSR IOREST     ;RESTORE CPU
9BEF- 40        2470          RTI
9BF0- 78        2480          SEI            ;DISABLE INTS
9BF1- 60        2490          RTS            ;SUB FOR BASIC
9BF2- 58        2500          CLI            ;ENABLE INTS
9BF3- 60        2510          RTS            ;SUB FOR BASIC
                2520 ;
                2530 ;
                2540 ;  TICK HANDLER SUB
                2550 ;
9BF4- AD A6 C0  2565 TICK     LDA STATUS+5   ;RESET CH3
9BF7- AD A7 C0  2566          LDA STATUS+6   ;INT BY READ
9BFA- CE 5F 9C  2567          DEC TCNT       ;TICK COUNTER
9BFD- D0 3E     2570          BNE ETICK      ;QUIT IF NOT DONE
9BFF- AD 5C 9C  2580          LDA INCNT      ;RESET COUNT
9C02- 8D 5F 9C  2590          STA TCNT       ;LOCATION
9C05- CE 60 9C  2600          DEC DCNT       ;DATA COUNT
9C08- D0 2D     2610          BNE ETICK1     ;NO SCAN YET
9C0A- AD 61 9C  2620          LDA DCNT+1     ;TEST HI BYTE
9C0D- F0 06     2630          BEQ DSCAN      ;DATA SCAN IF ZERO
9C0F- CE 61 9C  2635          DEC DCNT+1     ;DOWN TO ZERO
9C12- 4C 37 9C  2636          JMP ETICK1     ;QUIT
9C15- EE 63 9C  2640 DSCAN    INC DFLAG      ;SET SCAN FLAG
9C18- AD A2 C0  2641          LDA STATUS+1   ;SAVE RAD
9C1B- 8D 5B 9C  2642          STA HILATCH    ;IN COUNTER
9C1E- AD A3 C0  2643          LDA STATUS+2   ;GET LO COUNT
9C21- 8D 5A 9C  2644          STA LOLATCH    ;AND SAVE
9C24- A9 01     2645          LDA #RSTCMD    ;KILL PTM
9C26- 8D A0 C0  2646          STA CMDLOC     ;DURING SCAN
9C29- AD 5D 9C  2650          LDA DSAV       ;RESET DATA
9C2C- 8D 60 9C  2660          STA DCNT       ;LO BYTE
9C2F- AD 5E 9C  2670          LDA DSAV+1     ;AND HI BYTE
9C32- 8D 61 9C  2680          STA DCNT+1     ;FOR COUNT
9C35- D0 06     2690          BNE ETICK      ;NOW QUIT
9C37- EE 62 9C  2700 ETICK1   INC TFLAG      ;SET TEMP SCAN FLAG
9C3A- 20 00 9B  2701          JSR TSCAN      ;AND DO IT
9C3D- 60        2710 ETICK    RTS
                2720 ;
                2730 ;    PUMP SUB
                2740 ;
9C3E- AD A4 C0  2745 PUMP     LDA STATUS+3   ;RESET CH2
9C41- AD A5 C0  2746          LDA STATUS+4   ;BY READ
9C44- EE 59 9C  2750          INC PSTAT      ;BUMP IT UP
9C47- 60        2760          RTS            ;IS THAT ALL?
```

```
                    2770 ;
                    2780 ;  RADIATION SUB
                    2790 ;
9C48- AD A2 C0 2798 RAD     LDA STATUS+1 ;RESET  CH1
9C4B- AD A3 C0 2799         LDA STATUS+2 ;BY LATCH READ
9C4E- EE 57 9C 2800         INC LORAD    ;SO?
9C51- D0 03    2810         BNE ENDRAD   ;TEST FOR RECYCLE
9C53- EE 58 9C 2820         INC HIRAD    ;AND CARRY IT
9C56- 60       2830 ENDRAD  RTS          ;ALL DONE
9C57- 00       2840 LORAD   .DA #0
9C58- 00       2850 HIRAD   .DA #0
9C59- 00       2860 PSTAT   .DA #0
9C5A- 00       2870 LOLATCH .DA #0
9C5B- 00       2880 HILATCH .DA #0
9C5C- 0A       2890 INCNT   .DA #$A       ;INNER COUNTERPRESET
9C5D- 3C 00    2900 DSAV    .DA 60        ;OUTER COUNTERPRESET
9C5F- 0A       2901 TCNT    .DA #$A       ;INNER COUNT LATCH
9C60- 3C 00    2910 DCNT    .DA 60        ;OUTER COUNT LATCH
9C62- 00       2920 TFLAG   .DA #0        ;TEMP SCAN FLAG
9C63- 00       2930 DFLAG   .DA #0        ;DATA SCAN FLAG
                    2940 END
```